

ADDIS ABABA UNIVERSITY

ADDIS ABABA INSTITUTE OF TECHNOLOGY

SCHOOL OF GRADUATE STUDIES

SCHOOL OF CHEMICAL AND BIO ENGINEERING



**Modeling and Simulation of Reactive Distillation for Biodiesel
Production**

**A Thesis Submitted to the School of Graduate Studies of Addis Ababa
University, Institute of Technology, in Partial Fulfillment of the
Requirements for the Degree of Masters of Science in Chemical
Engineering (Process Engineering).**

By: Desalegn Ayalew

Advisor: Dr. Ing. Abubekir Yimam

February, 2015

Addis Ababa, Ethiopia

ADDIS ABABA UNIVERSITY

ADDIS ABABA INSTITUTE OF TECHNOLOGY

SCHOOL OF GRADUATE STUDIES

SCHOOL OF CHEMICAL AND BIO ENGINEERING



**Modeling and Simulation of Reactive Distillation for Biodiesel
Production**

**A Thesis Submitted to the School of Graduate Studies of Addis Ababa
University, Institute of Technology, in Partial Fulfillment of the
Requirements for the Degree of Masters of Science in Chemical
Engineering (Process Engineering).**

By:

Desalegn Ayalew

Advisor: Dr. Ing. Abubekir Yimam

February, 2015

Addis Ababa, Ethiopia

ADDIS ABABA UNIVERSITY

ADDIS ABABA INSTITUTE OF TECHNOLOGY

SCHOOL OF GRADUATE STUDIES

SCHOOL OF CHEMICAL AND BIO ENGINEERING

**Modeling and Simulation of Reactive Distillation for Biodiesel
Production**

By:

Desalegn Ayalew

Approved by the Examining Board:

Ato Taye Zewdu

Chair man, Graduate Committee

Signature

Date

Dr. Ing. Abubekir Yimam

Advisor

Signature

Date

Internal Examiner

Signature

Date

External Examiner

Signature

Date

Abstract

In this thesis, theoretical investigations have been made concerning reactive distillation columns. The detailed steady state modeling, and simulation are made for biodiesel produced by reactive distillation. This study was performed through several steps in order to construct and develop an improved steady state model based on recent manner of MESH equations (Mass balance, Equilibrium, Summation of composition, and Heat balance) the reaction portion added to the mass and energy balance. This model was developed to study the behavior of multi component non ideal mixture in reactive distillation. The set of algebraic equations governing steady state composition profile in a reactive distillation column are solved by using equation tearing or sequential method. The developed model can be employed to simulate the reactive distillation operation. This model required the in advance specification of number of reactive and non-reactive trays, the reflux ratio, composition and flow rates of the feed, and heat duty to determine the result of the liquid and vapor composition profiles, the temperature profile and the vapor and liquid flow rate profile. The validity of the developed steady state equilibrium model had been evaluated by comparing its predictions with another theoretical work. The calculations and simulations in this thesis were obtained by using MATLAB environment, version 10.

Acknowledgment

Praise is to GOD who gave me ability to achieve this research. I would like to thank all people who helped me during my research period. Foremost have been my **Advisors Dr.-Ing. Abubekir Yimam** and former **Advisor Dr.-Asfaw Gezae** ,I appreciate their guidance and suggestions they gave me during this work.

I would also like to express my acknowledgment to the staff of Chemical Engineering Department. Also great thanks are extended to all that helped me in one way or another; I wish to express my thanks.

And finally my special thanks go to my family for their support and encouragement.

Table of Contents

Contents	Page
Abstract	i
Acknowledgment.....	ii
Table of Contents.....	iii
List of Figures	vi
List of Tables	vii
Nomenclature	viii
1. INTRODUCTION.....	1
1.1. Biodiesel.....	1
1.2. Reactive Distillation.....	2
1.3. Problem Statement.....	2
1.4. Objectives	3
1.4.1. General Objective.....	3
1.4.2. Specific Objectives.....	3
2. LITERATURE REVIEW	4
2.1. Biodiesel Production	4
2.2. Characteristic of Biodiesel	5
2.3. Transesterification.....	5
2.4. Esterification	8
2.5. Reactive Distillation.....	11
2.5.1. Reactive Distillation Advantages	15
2.5.2. Constraints and Disadvantages of Reactive Distillation	16
2.5.3. Commercial Applications of Reactive Distillation Include Following	17

2.6.	Modeling and Simulation of Reactive Distillation.....	18
3.	REACTION, PHYSICAL AND THERMODYNAMICS PROPERTIES.....	20
3.1.	Introduction.....	20
3.2.	Reaction Kinetics	20
3.3.	Physical and Thermodynamics Properties.....	22
3.3.1.	Thermodynamics Properties.....	22
3.3.2.	Physical Properties	24
3.4.	Vapor- Liquid Equilibrium.....	27
3.5.	Enthalpy	29
4.	MATHEMATICAL MODEL DEVELOPMENT.....	31
4.1.	Introduction.....	31
4.2.	Modeling of Reactive Distillation.....	31
4.3.	Equilibrium Stage Model	32
4.4.	Solution Method.....	36
4.4.1.	Initial Condition.....	36
4.4.2.	Initial Estimation.....	37
4.4.3.	Computational Algorithms for Reactive Distillation	38
4.4.4.	Equation – Tearing or Sequential Procedures.....	39
4.5.	Degree of Freedom Analysis.....	42
4.6.	Bubble Point Method for Distillation	44
4.7.	Simulation by MATLAB	49
5.	RESULT AND DISCUSSION.....	50
5.1.	Introduction	50
5.2.	Validation of Simulation Results	51
5.3.	Simulation of concentration profile	52

5.4. Simulation of Temperature Profile.....	55
5.5. Sensitive Analysis.....	56
5.5.1. Effect of Reflux Ratio	56
5.5.2. Effect of Trillion Feed Concentration.....	58
5.5.3. Effect of Feed Temperature	59
5.6. Liquid and Vapor Flow Rate	60
6. CONCLUSION AND RECOMMENDATION.....	62
6.1. Conclusion.....	62
6.2. Recommendation for Future Work	63
REFERENCE.....	64
APPENDICES	68
A: Matlab Scripts	68
B: Estimation of Critical Temperatures and Pressures.....	75
C: Bubble Point Estimations	77
D. Estimation of Vapor Pressure Equations	79

List of Figures

Figure 2.1. Transesterification reactions.	6
Figure 2.2. Schematic representation of a conventional and reactive distillation process (Around, 1999).	14
Figure 4.1. (a) Multi-stage distillation column. (b) The equilibrium stage.	33
Figure 4.2. Flow Chart of Simulation Program for Continuous Reactive distillation.	47
Figure 5.1. A modified flow sheet of the reactive distillation process from Simasatitkul et al.[1]	50
Figure 5.2. The liquid concentration of methyl linoleate under simulation results from thesis work vs results from Emile’s work.	52
Figure 5.3. Concentration profile for vapor phase using equilibrium model.	53
Figure 5.4. Concentration profile for liquid phase using equilibrium model.	54
Figure 5.5. Temperature profile for equilibrium model.	55
Figure (5.6a) Liquid composition profile with reflux ratio =4.	57
Figure (5.6b) Liquid composition profile with reflux ratio =5.	57
Figure 5.7. Variation of trillion conversions with trillion concentrations in the feed stream using equilibrium model	58
Figure 5.8. Effect of feed stream temperature on conversion.	59
Figure 5.9. liquid flow rate along stage of the column	60
Figure 5.10. Vapor flow rate along stage of the column	61

List of Tables

Table 2.1. Overview of the different processes for producing biodiesel [5].....	10
Table 3.1 The kinetic parameters for the transesterification reactions [1].....	21
Table 3.2. The parameters of vapor pressure [9].....	22
Table 3.3. Constants for heat capacity.....	23
Table 3.4: Physical and thermodynamic properties of the biodiesel compounds [9], [21], [20].....	24
Table 3.5. Temperature Dependant properties of TG, GL, MetOH and BD [9].....	25
Table 3.6: Temperature dependent propeties for DG and MG.....	26
Table 3.7. Useful expressions for estimating K-values for vapor-liquid equilibria [18]....	27
Table 3.8. The values of relative volatilities of TG, DG, MG, GL and BD with respect to Methanol.....	28
Table 3.9. : Molar heat of formation of component.....	30
Table 4.1. Initial conditions for the reactive distillation of biodiesel from Simasatitkul et al.[1].....	36
Table 4.2. Number of variables and equations.....	43
Table 5.1. Operational condition and column specification for the reactive distillation simulation.....	51
Table 5.2. Comparison between results obtained in this work and those by Emilie Øritsland Houge et.al (2012).....	51
Table B-1: Group contributions to <i>T_c</i> and <i>P_c</i>	76
Table C-1: The heats of formation and heat of condensation for methanol and trillion....	78

Nomenclature

A	Arrhenius frequency factor
A,B,C,D,E	modified Antoine parameters
C	number of components
C_{p_l}	Liquid heat capacity [J/mol. K]
E	activation energy [J/mol]
E_{MV}	Murphee coefficient
F	feed flow rate (kmol/s)
f	component feed flow rate [mol/s]
H_f	heat of formation [J/mol]
ΔH_{vap}	Standard heat of vaporisation [kJ/kmol]
L_j	liquid flow rate [kmol/s]
N	number of stage
P	total pressure [Pa]
P_c	critical pressure [Pa]
Q_j	heat duties [J/s]
R	universal gas constant [J/mol.K]
P^*	modified Antoine pressure [Pa]
$R_{m,j}$	rate of reaction m, on stage j [mol/s]
$\Delta R_{i,j}$	rate of consumption of i on stage j [mol/s]
dR_m	total rate of reaction of consumption on stage j [mol/s]

T	temperature [K]
T_b	boiling point temperature [K]
T_c	critical temperature [K]
T_r	reduced temperature [K]
V_j	vapor flow rate [kmol/s]
$x_{i,j}$	mole fractions of component i for liquid flow on stage j .
$y_{i,j}$	mole fractions of component i for vapor flow on stage j .

Greek symbol

α	relative volatility
γ_i	liquid activity coefficient
ϕ_i^0	vapor fugacity coefficient
ϕ_i^v	vapor fugacity in a mixture
ρ	density [kg/m^3]
ϵ	reaction volume [m^3]
ν_{im}	stoichiometric coefficient of i in reaction m .

Subscripts

i	component index
j	stage index
m	reaction index
t	total

Superscripts

F referring to feed stream

L referring to liquid phase

V referring to vapor phase

Abbreviations

AIChE American institute for chemical engineers

BD biodiesel

CH₃O⁻ methoxide

DG diglyceride

FFAs free fatty acids

GL glycerol

MetOH methanol

MG monoglyceride

OH⁻ hydroxide ion

RD reactive distillation

1. INTRODUCTION

1.1. Biodiesel

The diesel fuel derived from petroleum has played an important role in the industrial development. Its low cost causes it to be used to mobilize the charge transport, the transport of passengers in big cities and in the generation of electrical energy. However, it is a non-renewable resource; the gases of its combustion generate high environmental problems. That is why in the last decade an alternative for obtaining diesel has been looked for. For this reason a series of investigators tries to obtain biodiesel by transesterification of vegetables oils with alcohol (Srivastava and Prasad, 2000).

Biodiesel is an alternative diesel fuel made from vegetable oils by transesterification reaction with a short chain alcohol. The main advantages over regular diesel are that it is biodegradable, low toxicity, it produces lower emissions, it is environmental friendly (Ma and Hanna, 1999), it has higher flash point (making it safer to handle and store) and it is a better lubricant (Kiss et al., 2007). It has similar properties compared to diesel produced from crude oil and it can be used in its pure form or as a diesel/biodiesel mixture on existing fuel engines. However, it is still more expensive than conventional diesel (Behzadi and Farid, 2009).

It has been known that the transesterification of vegetable oils to fatty acid ester as a biodiesel is an equilibrium-limited reaction. A large excess of alcohol over a stoichiometric ratio is usually employed in conventional reactors to achieve a high degree of the conversion of vegetable oils, thereby requiring the expensive separation of unreacted reactants from the biodiesel product. As a consequence, potentially alternative processes to overcome such a difficulty should be explored. When considering the characteristics of the transesterification reaction, the use of reactive distillation, a multifunctional reactor combining chemical reaction and distillation in a single column is becoming more important.

1.2. Reactive Distillation

The reactive distillation is a hybrid process that combines the reaction and separation in a single column where the products are being continuously removed. This characteristic made possible to overcome the thermodynamic equilibrium limitations of the reaction, reaching best conversion and selectivity (Pai et al, 2002; Pisarenko et al, 2001).

Reactive distillation (RD) is the process in which chemical reaction and separation are carried out simultaneously within a fractional distillation apparatus. It may be advantageous for liquid-phase reaction systems when the reaction must be carried out with a large excess of one or more of the reactants, when a reaction can be driven to completion by removal of one or more of the products as they are formed, or when the product recovery or by-product recycle scheme is complicated or made infeasible by azeotrope formation (Perry *et al.*, 1997).

1.3. Problem Statement

Petroleum products mainly gasoline and diesel have played important role in the world nowadays not only in economics, but also in the industrial development. However, they are not renewable source and contribute to the unwanted effect to the world environment.

Thus, biodiesel are the best renewable energy replacement for diesel from petrol, which did not cause sulfur contaminant. Recently, the biodiesel production from various oil sources is produced using common reactor and distillation system. However, this conventional system in making biodiesel leads to higher equipment and maintenance costs, byproduct production and energy consumption.

Reactive distillation can substitute the conventional reactor and distillation system, which not only potentially reduce the space and cost for equipment and maintenance, but will be able to overcome or breaking the reaction thermodynamic equilibrium limitation to obtain higher conversion of desired product.

1.4. Objectives

1.4.1. General Objective

The main aim of the research is to model and simulate the production of biodiesel from vegetable oil by reactive distillation.

1.4.2. Specific Objectives

The specific objectives of the research are:

- ❖ To develop a reactive distillation model for biodiesel production process from vegetable oil.
- ❖ To develop rigorous mathematical model for biodiesel production in a reactive distillation column for both steady state and dynamic conditions
- ❖ Developing computer programs, MATLAB or/and C++, to solve the resulting equations
- ❖ To determine the optimum process parameters to achieve highest conversion of product
- ❖ Sensitive analysis for the effects of process parameters

Thesis outline

Chapter 1 provides an introduction to biodiesel and reactive distillation. The objectives of the thesis have been stated. Chapter 2 presents a brief literature related to biodiesel and reactive distillation. Chapter 3 discusses the thermodynamics, kinetics and physical properties of the system under study. Chapter 4 includes a detailed approach for the simulation, the mathematical modeling for reactive distillation column and the solution methods. In chapter 5 the simulation results obtained are validated, and discussed. The simulation results of the equilibrium model are compared. Chapter 6 summarizes the conclusions reached during the course of this study.

2. LITERATURE REVIEW

2.1. Biodiesel Production

Biodiesel is vegetable or plant-based oils that can be used as fuels, and normally consists of long chain alkyl esters. The first use of vegetable oils as fuels was demonstrated by Rudolph Diesel, the inventor of the diesel engine in the start of the 20th century. He was of the opinion that vegetable oils were the fuel of the future [5]. However, because of the cheap fossil fuel prices, biodiesel was not considered a viable alternative until recently, when fossil fuel prices have increased and are estimated to keep rising [3]. Biodiesel is promising in that it represents an environmentally friendly alternative or additive to regular fossil fuels that can be used on present engines with no or little modification. Biodiesel can also improve the performance of the engine and even prolong the engines' life as it showcases both increased solvent effect and lubrication properties [5].

The world's oil supply is anticipated to deplete by 2060 due to the increase in demand for energy coupled with depletion of petroleum oil [1]. Therefore, seeking for a sustainable energy pathway to meet the energy needs of the future generation is desirable.

Biodiesel is renewable, nontoxic, biodegradable, and essentially free of sulfur and aromatics may be one of the most suitable candidates for future biofuel. Beside, U.S. Department of Energy life cycle analysis on biodiesel shows that biodiesel produces 78.5% less net carbon dioxide emissions compared to petroleum diesel [2]. In 2011, the United States produced approximately 1.1 billion gallons of biodiesel and the volume of production is expected to increase to 1.9 billion gallons in 2015 [3]. Major drawbacks of biodiesel production using vegetable oil are the cost of manufacturing and the high cost of oil since it competes with food. Currently, biodiesel production plants depend on government subsidies in order to keep their plants in operation. Thus, seeking for a more economic biodiesel production process to reduce the dependency of government subsidies and promote expansion of biodiesel industry is desirable.

Biodiesel is an alternative diesel fuel that is produced from vegetable oils and animal fats. There are many methods to produce biodiesel such as esterification, transesterification,

pyrolysis, supercritical reaction and lipase-catalyzed for biodiesel production which transesterification methods give biodiesel grade near diesel.

2.2. Characteristic of Biodiesel

Biodiesel was well known as an alternative fuel for diesel engines that is chemically produced by reacting the virgin or used vegetable oil or animal fats with an alcohol such as methanol in order to accelerate the reaction (Leung et al, 2006).

Biodiesel colors can be varied between golden and dark brown because it depends on the production feedstock. It is practically immiscible with water, has high boiling point (475K (>2020C)) and low vapor pressure. Typical methyl ester biodiesel has a flash point of ~150°C (300°F), making it rather non-flammable. Biodiesel has density of ~0.88g/cm³, less than water. Biodiesel that unpolluted with starting material can be regarded as non-toxic. It also has similar viscosity with petro-diesel that produces from petroleum.

Moreover, biodiesel is also clean burning diesel fuel replacement made from natural, renewable source, such as new and used vegetable oils or animal fats. It will run in any diesel engine with a little or no modification and can be mixed with regular diesel fuel in any ratio. Biodiesel is non-toxic and biodegradable.

2.3. Transesterification

Transesterification is a reaction between a triglyceride and an alkyl alcohol, producing alkyl esters (biodiesel) and glycerol. Figure 2.1 below depicts the transesterification reaction.

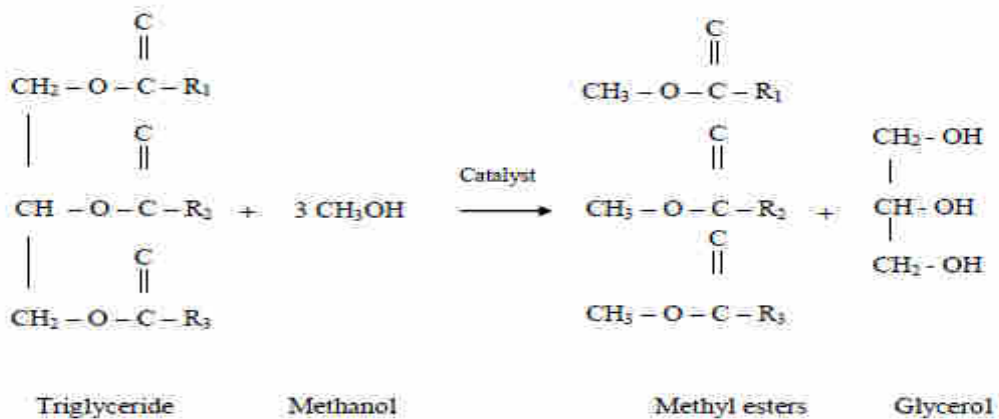


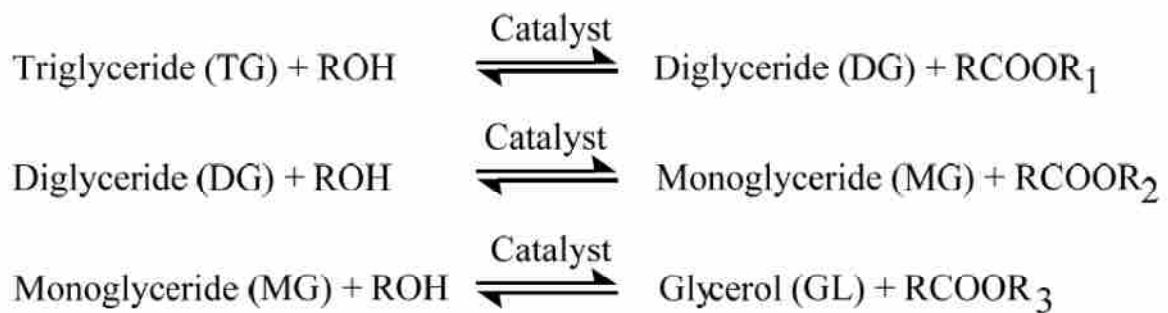
Figure 2.1. Transesterification reactions.

One mole of triglyceride reacting with three moles of methanol produces three moles of methyl esters and one mole of glycerol.

Transesterification is chemical reaction between triglyceride, alcohol with catalyst to produce biodiesel and glycerol. The catalyst is used in this method that can be classified as two groups. One is homogeneous catalyst and the other is heterogeneous catalyst. The both type catalyst, there are several kinds; alkali catalyst, acid catalyst, lipases (biocatalyst). These two catalysts are advantage and disadvantage. Producing biodiesel via homogeneous is fast reaction and give high conversion biodiesel but cannot recovery catalyst for next times. If choosing production biodiesel via heterogeneous catalyst, it can be solve problem of homogeneous catalyst and suitable for manufacturing industry.

Transesterification consists of 3 steps in series with 2 intermediates namely diglycerides (DG) and monoglycerides (MG). The steps are shown in Figure 2.2. The alcohol used in transesterification is a short type such as methanol, ethanol, propanol and butanol. However, methanol is the favorite choice since its low cost and physical and chemical advantages (polar and shortest chain alcohol). For the stoichiometry of transesterification, the ratio of alcohol to oil is 3:1 but an excess of alcohol is usually used in order to shift the reaction for more production of biodiesel.

The overall reaction consists of 3 stepwise with intermediate formation of diglycerides (DG) and monoglycerides (MG). The 3 step reactions are shown in the Figure 4. The alcohols that can be used in the transesterification reaction are methanol, ethanol, propanol and butanol. Methanol is usually used because of low cost and its physical and chemical advantages (polar and shortest chain alcohol). The stoichiometric between alcohol and the oil is 3:1. However, an excess of alcohol is usually more in order to shift the reaction to the right hand side.



Transesterification is the reaction between vegetable oils or animal fats with alcohol to produce ester and glycerol by using catalyst such as base catalyst, acid catalyst, lipase and heterogeneous catalyst.

The mechanism of alkali catalyst transesterification with vegetable oil (Schuchardt et al., 1997) is shown in the Figure 4. There are consists of three steps. The first step is an attack on the carbonyl carbon atom by the methoxide ion (CH₃O⁻) to form a tetrahedral intermediate. In the second step, the tetrahedral intermediate reacts with an alcohol (methanol) to regenerate the anion of the alcohol. In the last step, rearrangement of the tetrahedral intermediate results in the formation of a fatty acid ester and a diglyceride. Diglycerides and monoglycerides are converted by the same mechanism to a mixture of alkyl esters and glycerol.

The advantages and disadvantages of each catalyst are described below. The advantages of homogeneous catalysts are the rapid reaction, high conversion. However, the disadvantages of homogeneous catalysts are saponification reaction, difficult separation

between biodiesel and catalyst. Therefore the heterogeneous catalyst is studied to reduce the problem in biodiesel production because the biodiesel using heterogeneous catalyst is easy to separate between catalyst and glycerin.

Firstly, the common homogeneous are acid and alkali catalyst. Using alkali catalysts, the reaction is fast, high conversion and less corrosive than acid compound. However, hydroxide ion (OH⁻) of alkali catalyst can react with the free fatty acid to produce soap. The soap formation is an undesirable side-reaction, because it partially consumes the catalyst, decreases the biodiesel yield and complicates the separation and purification steps (Vicent et al., 2003). The removal of these catalysts is technically difficult and brings extra cost to the final product. In addition, the difficulty for recycling and the generation of large waste amounts make the traditional catalysts less favorable. The soap formation can be suppressed by using acid catalyst because there is no hydroxide ion. The acid reacts with free fatty acid to produce fatty acid esters, increasing the biodiesel yield. Nevertheless, the reaction of acid catalyst is lower than the acid and also needs more extreme temperature and pressure conditions.

Although, chemical transesterification using alkali catalyst process gives high conversion in small time. But it is difficult to removed glycerin and requires the waste water treatment. Therefore, using lipase as catalyst can overcome these problems. In addition, there are many advantages such as:

- ❖ Possibility of regeneration and reuse
- ❖ Lower temperature of reaction
- ❖ Higher biodiesel

However, production cost of lipase catalyst is expensively than alkaline one. Furthermore, other technique to produce biodiesel is transesterification using supercritical fluids. Saka and Kusdiana (2001) studied biodiesel production in super critical methanol. They demonstrated that preheating to 350 °C and treatment for 240 s during the reaction. The biodiesel has a higher than conventional method using base catalyst. However, the

supercritical methanol method requires a high temperature of 350 °C and a pressure of 45 MPa, and in addition, large amount of methanol is necessary.

2.4. Esterification

The esterification reaction is used for raw materials that have a modest to high degree of free fatty acids such as waste cooking oil. This reaction converts the free fatty acids to alkyl esters in one single step, and normally employs an acid catalyst such as HCl or sulphuric acid. Because it is uncommon to have only FFAs present in a raw material source, it is normal to have the transesterification and esterification reactions occur simultaneously to target both the free fatty acids and the TAGs at the same time, or to use the esterification process as a pre-treatment step before the transesterification reaction [5].



There are two known competing reactions to the biodiesel production, called the saponification (soap-formation) reaction, and the hydrolysis reaction. These are shown below as equations 2.3 and 2.4 [5].



Both of these reactions are unwanted and may propose difficulties with cleaning the equipment, and dilution of the product, deactivation of the catalyst and interference with the main reaction. The saponification and hydrolysis reactions depend on the presence of free fatty acids (FFAs), but research has shown that if the amount of FFAs is less than 0.5% the reduction in reaction efficiency is negligible [12].

There are several process for producing biodiesel, such as batch, continuous, enzymatic, supercritical and reactive separation [6]. The advantages and disadvantages of each process are described below in Table 2.1.

Table 2.1. Overview of the different processes for producing biodiesel [5].

Process	Advantages	Disadvantages
Batch	Good flexibility with regard to feed composition	Low productivity and high Operational costs.
Continuous	Combination of transesterification and esterification reaction which leads to high productivity.	Normally uses homogeneous Catalysts, which means it is subject to corrosion and extensive cleaning is necessary.
Supercritical	No catalyst and no hindrance to the transesterification kinetics due to oil alcohol miscibility.	Severe conditions that require special equipment (costly).
Enzymatic	Low energy requirements.	Low yields and productivity, long reaction times.
Multistep	Applies both transesterification and esterification. High purity glycerol is obtained as a byproduct. Solid catalyst can be used.	High capital costs
Reactive distillation	High conversion and yields, reduced post-processing	Damage of equipment if combined with homogenous catalysts

Strong incentives for efficient production of renewable fuels have shifted the interest to larger scale production of biodiesel. Because of this, the processes mostly used in industry today are the multistep and the continuous method. The enzymatic method and the

supercritical method show promise but do not offer enough of an economic advantage to be applied commercially at the time being [6].

A lot of research is being developed on reactive separations at the present and this group consists of: reactive distillation, reactive absorption, membrane reactors and reactive extraction. Reactive distillation is the reactive separation process with the most applications, the focus of this paper and is explained in more detail in the next section [6].

2.5. Reactive Distillation

Reactive distillation is a hybrid unit which comprises distillation and reaction in a single unit operation. Recently reactive distillation has become a strong interest in chemical engineering research, although the concept of reactive distillation has been known for a long time. In the 1920's the technique was applied to esterification processes using homogeneous catalysts (Backhaus, 1921). In 1971, Sennewald described a development employing solid heterogeneous catalysts. The most important benefit of reactive distillation lies in the economics: a reduction in capital cost, energy saving, raw materials and solvent reduction. By carrying out distillation and chemical reaction in the same unit, one process step is eliminated, along with the associated pumps, piping and instrumentation. This gives safer environmental performance (the area or scale of risk and hazards is significantly reduced with just one continuous operating unit) as well as better energy management (the heat of reaction creates more boil-up and better vapour-liquid phase transfer, but no increase in temperature; therefore, no cooling is required). Particularly good candidates for reactive distillation are processes in which the chemical reactions are characterized by: unfavorable reaction equilibrium: all chemical reactions have an equilibrium reaction. There are chemical reactions for which, at operating temperature, the mixture at chemical reaction equilibrium conditions still contains considerable concentration of reactants. Even if one of the reactants is present in a high concentration the reaction will not proceed. Such reactions are normally so-called equilibrium-limited. For these chemical reactions the conversion can be increased by continuous removal of products from the reacting mixture. High heat of reaction: some chemical reactions have large heat of reaction (exothermic or endothermic). If these

reactions occur in reactors they will change the temperature and modify the reaction progress. In reactive distillation the heat of reaction will not modify the temperature, the phases will remain at the boiling point, and the heat of reaction will not affect the reaction equilibrium. In the case of exothermic reactions, the heat of reaction is directly used for the distillation process. Large excess of reactants required: reactive distillation is also potentially attractive whenever a liquid phase reaction must be carried out with a large excess of one reactant. In this situation, conventional processes need large recycle cost (for the excess of reactant); however, reactive distillation could be carried out closer to stoichiometric conditions minimizing the recycle cost.

Reactive distillation prevents side reactions and overcomes limitations due to chemical equilibrium by its natural separation. Azeotropic conditions: reactive distillation can overcome the limitations imposed by azeotropic mixtures: simultaneous chemical and phase equilibrium has the most beneficial effect of reacting away some of the azeotropes and thereby, simplifying the phase behavior. Systems with solid catalysts: reactive distillation is especially applicable to a certain class of reactions that employ solid catalysts. The important points that characterise the catalyst systems are the activity of the catalyst at distillation conditions and the relative volatility of the reactants and products.

The balance between these two characteristics makes some chemical systems perfect candidates for this technique. The main disadvantage of reactive distillation is that it is highly system specific and its suitability needs to be assessed separately for each process.

Reactive distillation has a strong dependency on the properties of the chemical system that is dealt with. The poor knowledge of the chemical reactions features, (catalyst, kinetics, hold-ups) and distillation (vapour-liquid equilibria, thermodynamics, plate and/or packing behaviour) together with their combination in a reactive distillation unit, makes such a unit difficult to simulate and operate.

Reactive distillation appears to be an interesting process unit. Models capable of dealing with different processes are still not available. Although fully equilibrium considerations may give the limits for reaction and separation, reactive distillation columns will not operate at equilibrium (real operations are not at equilibrium).

The reactive distillation is an operation which reactions and separations taking place in the same unit. This technique is especially useful for equilibrium-limited reactions such as esterification and ester hydrolysis reactions. Conversion can be increased far beyond the equilibrium due to the continuous removal of products from the reactive zone. This approach can potentially reduce capital investment and operation costs.

The integration of unit is an interesting:

1. simplification or elimination of separation system can lead to capital savings,
2. conversion can be increased by removing production continuously
3. The azeotropes mixture can prevent by using reactive distillation instead of reactor and distillation
4. Removing one of the products from the reaction mixture can lead to reduction the rates of side reactions and by product formation
5. If the reaction is exothermic, the heat of reaction can be used to provide the heat of vaporization that reduces the reboiler duty

As previous mentioned, using the reactive distillation can reduce capital investment such as the production of methyl acetate. The acid catalyst reaction (methanol react with acetic acid to produce methyl acetate and water) was traditionally carried out by using the processing scheme as seen in the Figure 4(a). In this figure, there consists of one reactor and nine distillation. Figure 4(b) shows the reactive distillation implementation, only one column is required. The capital and operation costs are reduced (Siirola, 1995).

The potential benefits of applying RD processes are taxed by significant complexities in process development and design. For reactions that are irreversible, it is more economical to take the reaction to completion in a reactor and then separate the products in a separate distillation column (Harvey, 2004).

The principles may be illustrated when we look for an example process for the production of chemical C out of A and B according the following reaction scheme:



In addition some undesired side reactions are assumed, such as for example:



This reaction can be carried out in a conventional process setup as sketched on Figure 1(i); the objective is to produce C out of reactants A and B, thereby making byproduct D. In addition, there are undesired side and consecutive reactions, so that the exit stream of the reactor will be a mixture of all components.

A and B have to be separated and recycled, C has to be separated and purified to separation, and D, E, and F have to be disposed of. Normally, this will require more than the single distillation column that is given in Figure (2.2). Shown on the right hand side of Figure (2.2) is a typical setup for reactive distillation column. The reactions will take place in the reactive section.

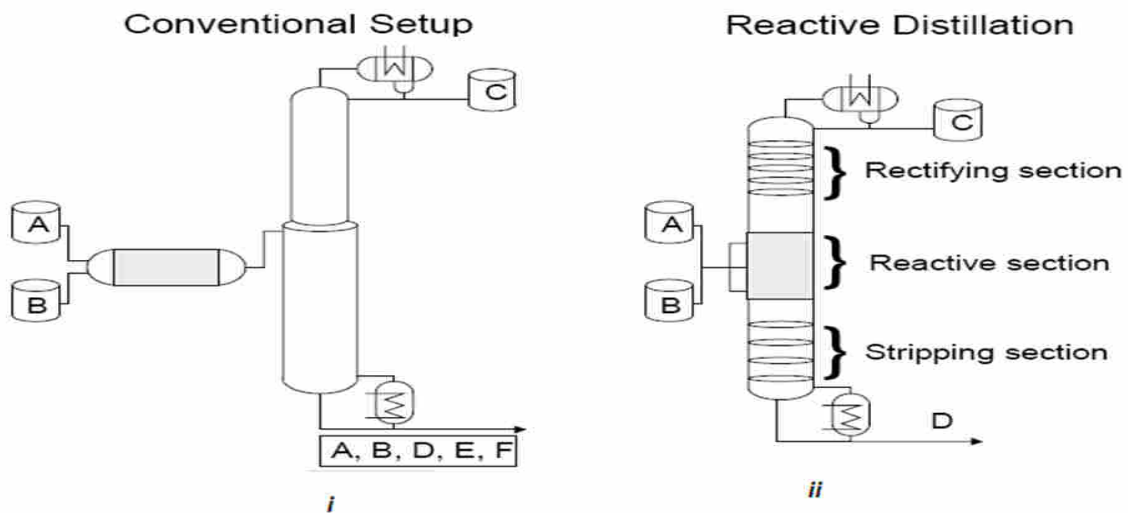


Figure 2.2 Schematic representation of a conventional and reactive distillation process (Around, 1999).

In case of a heterogeneous reaction, this section can consist of reactive packing elements but also of trays that are covered with a teabag type. For homogeneous reactions, the

location of the reactive section is defined by the feed location of a homogeneous liquid catalyst. The non-reactive rectifying and stripping section take care of additional product separation. In this kind of setup there is in-situ product removal of desired product C, which will pull the equilibrium of the main reaction towards the right hand side, thereby increasing the overall conversion. This way one can overcome a bad equilibrium constant. In addition, lowering the concentration of C due to the in-situ separation will also reduce the rates of side reactions, there will be less conversion of C to undesired side products, and this illustrates how reactive distillation may be applied to systems where selectivity is important.

The non-reactive section in the column play an important role in product separation and reactants recycle. In the ideal case, the non-reactive zones separate the products from the reactant in such a way that the reactants are automatically flushed back into the reactive zone, while pure products may be obtained as product stream. The design and operation issues for reactive distillation (RD) system are considerable more complex than those involved for either conventional reactor or conventional distillation column.

2.5.1. Reactive Distillation Advantages

The advantages and constraints in reactive distillation are specific to each system. The advantages of reactive distillation in general are:

1. Chemical equilibrium limitation can be overcome, an equilibrium reaction can be driven to completion by separation of products from the reacting mixture (i.e., reaction conversion can approach 100%). Higher conversions are obtained due to shifting of the equilibrium to the right. This is exemplified by the production of methyl acetate. (Stankiewicz, 2003; Agreda et. al., 1990) and tertiary amyl ether (Bravo et. al., 1993).
2. Higher selectivity can be achieved elimination of possible side reaction by removal of the product from the reaction zone. This can serve to increase selectivity. In some applications particularly in cases when thermodynamic reaction prevents high conversion the coupling of distillation to remove reaction product from reaction

zone can improve the overall conversion and selectivity significantly, for example in the production of propylene oxide from propylene chlorohydrins (Carra et. al., 1979) and for alkylation of benzene to produce cumene (Shoemaker and Jones, 1987).

3. Improvement quantity of used materials. For example, it may be possible to operate with a reduction in the amount of excess reactant fed to the reactor. Normally feeding one reactant in excess is used to shift the equilibrium towards the production of product. With reactive distillation, this shift is attained through removal of the reaction products from reaction phase. Also elimination by-product formation may allow the use of lesser quantities of reactant. It may also be possible to avoid auxiliary solvent.
4. The heat of reaction can be used in-situ for distillation, saving associated energy costs, through use of energy released by exothermic reaction for vaporization. This reduces the reboiler heat duty which is supplied normally by steam. Benefits of heat integration are obtained because the heat generated in chemical reaction is used for vaporization, this particularly advantageous for situation involving heat of reaction such the hydration of ethylene oxide (Circ et. al., 1994).
5. Reduction of hotspot, because the liquid vaporization provides a sink for thermal energy. This is beneficial in, for example, the hydrolysis of ethylene oxide to ethylene glycol (Circ et. al., 1994).

2.5.2. Constraints and Disadvantages of Reactive Distillation

In spite of above stated benefits of reactive distillation, cannot be used for every process that requires reaction and separation in a single unit. It has some constraints. In general, reactive distillation is not attractive for supercritical condition, for gas-phase reaction, and for reaction that must take place at high temperature and pressures, and/or that involves solid reactants or products [1].

This type of reactive distillation is considered as an alternative to the use of separate reactor and distillation vessel whenever the following holds:

1. Feasible temperature and pressure for the reaction and distillation are the same. That is, reaction rates and distillation rates are of same magnitude. The reactions have to show reasonable data for conversions at pressure and temperature levels that are compatible with distillation conditions.
2. The chemical reaction occurs in the liquid phase, in the presence or absence of a homogeneous catalyst, or at the interface of a liquid and a solid catalyst.
3. The reaction is equilibrium-limited such that if one or more of the products formed can be removed, the reaction can be driven to completion; thus, a large excess of a reactant is not necessary to achieve a high conversion. This is particularly advantageous when recovery of the excess reagent is difficult because of azeotrope formation.
4. Higher requirements on the quality of the design and control systems including more sophisticated controller designs and more complicated control structures
5. Residence time requirements but limited hold-up in distillation column
6. Volatility constraints for reagents and products in the reaction zone of distillation column

2.5.3. Commercial Applications of Reactive Distillation Include Following

1. The esterification of acetic acid with ethanol to produce Ethyl acetate and water.
2. The reaction of formaldehyde and methanol to produce methyl and water, using a solid acid catalyst, as described by Masamoto and Matasuzaki.
3. The esterification of acetic acid with methanol to produce methyl acetate and water, using sulfuric acid as catalyst, as patented by Agreda and Partin, and described by Agreda, Partin and Heise.
4. The reaction of isobutene with methanol to produce methyl-tert-butyl ether (MTBE), using a solid, strong-acid ion-exchange resin catalyst, as patented by Smith and further developed by DeGarmo, Parulekar, and Pinjala.

There are many documented success stories involving the industrial implementation of reactive distillation. The applications of reactive distillation in the chemical and petroleum industries have increased rapidly in the past decade. One such example is the manufacturing of methyl acetate by the Eastman Chemical Company. In this case a single reactive distillation column replaced the traditional flow sheet consisting of eleven major unit operations along with an assortment of heat exchangers, pumps and controllers. The result was a five- fold reduction in capital investment and energy consumption over the conventional design for methyl acetate production.

2.6. Modeling and Simulation of Reactive Distillation

Several models have been published for biodiesel reactions and processes. The kinetic models of both esterification and transesterification reactions establish the order of the reaction, catalytic effect and the effect of temperature. Most acid catalyzed esterification kinetic models were pseudo-first order with respect to free fatty acid for the forward reaction of esterification and second order for the reverse reaction (13). Alkaline transesterification of triglycerides has been observed to be pseudo-second order initially followed by a shift to first or zero order kinetics (17). Nouredini and Zhu (1997) (46) proposed and solved an extended kinetic model of Freedman et al. (47) for alkaline transesterification of soybean oil where they reported rate constants for two different agitation regimes (based on Reynold's number). They also fit the model based on second order kinetics with and without a shunt reaction scheme.

Kinetic mechanisms have been proposed in the context of producing biodiesel through process intensification. Immobilized enzyme catalysis models have been proposed and combined with experiments to estimate parameters and can be used to optimize and design scaled-up bioreactors for biodiesel production. A –Ping-Pong Bi mechanism for the kinetics of lipase enzymes with competitive reactant inhibition correctly describe the kinetics of transesterification of palm oil with methanol catalyzed by the lipase from *M. mieheii* in *n*-hexane micro-aqueous system (26). The same model was lumped with mass transfer limitations in a dynamic model for transesterification to study biodiesel production from waste cooking oil.

Mass transport and kinetic parameters were determined by comparison with experiments and the model was found to fit the data well. It led to find that methanol inhibits the reaction more than the triglyceride substrate (17). Cheirslip et al (2008) (48) developed three kinetic mechanisms and corresponding models for lipase catalyzed transesterification of palm oil fatty acids. The model was use to estimate parameters by fitting with experimental data. They found that the hydrolysis and ethanolysis proceeds simultaneously and that all the species affects the reaction rate.

The literature review on distillation has been extensively addressed in the past. Several books offer the possibility of understanding as well as showing how to model, design and control a distillation unit.

Examples are, King (1980), Kister (1990, 1992), Luyben (1974), Skogestad and Postlethwaite (1996), to name a few. For this reason we have focused here on the description of the research over the years of only reactive distillation columns.

In recent years a large number of computational algorithms have been reported to solve the mass and energy balance equations together with the phase equilibrium data describing the reactive distillation problem. The unknown variables determined by solving these equations are mole fractions of phases, stage temperatures, rate of reaction and flow-rates of each phase. The equilibrium model is the standard model for simulating reactive or non-reactive distillation. The key assumption in these models is that the vapor and liquid leaving a reactive or non-reactive stage are in equilibrium and both temperatures (liquid and vapor) on the stage are assumed equal.

3. REACTION, PHYSICAL AND THERMODYNAMICS PROPERTIES

3.1. Introduction

Modeling and simulation of chemical processes need accurate and reliable estimation of the properties of the mixtures present in the process. In these situations the property models are in a service role where they supply the need properties only when requested. Due to the solution procedures employed in simulation, the property models are required to develop.

3.2. Reaction Kinetics

Reactive distillation involves simultaneous chemical reaction and separation. The chemical reaction usually takes place in the liquid phase or at the surface of a solid catalyst in contact with the liquid phase. Therefore, models for the reaction kinetics are important to consider. It is possible to obtain the desired product without the need for additional distillation for multi-component systems.

The model is focused on the main ester of soybean oil; trilinolein. Trilinolein will react to form biodiesel through the transesterification reaction. The consecutive steps of transesterification reaction are given below as reactions (5).



Here the first rate constant for each reaction constitutes the rate constant for the forward reaction while the latter represents the rate constant for the reverse reaction. The values for the rate constants and the activation energies of the reactions (3.1 -3.3) are given in

table 3.1, in the form of the Arrhenius equation which is displayed below as equation 3.4[23].

$$k_i = A_i \cdot \exp \left\{ \frac{E_i}{RT} \right\} \quad (3.4)$$

Table 3.1 The kinetic parameters for the transesterification reactions [1].

Rate constant	A(m ³ mol ⁻¹ h ⁻¹)	E(J mol ⁻¹)
k_1	1.4040 * 10 ¹¹	54.999
k_2	2.0808 * 10 ⁹	41.555
k_3	2.1262 * 10 ¹⁶	83.094
k_4	3.5597 * 10 ¹³	61.250
k_5	1.9206 * 10 ⁷	26.865
k_6	7.5600 * 10 ⁷	40.116

The equations for the rate of change per species are shown below, developed from the rate law [23].

$$r_{TG} = -k_1 [TG][MetOH] + k_2 [DG][BD] \quad (3.5)$$

$$r_{DG} = k_1 [TG][MetOH] - k_2 [DG][BD] - k_3 [DG][MetOH] + k_4 [G][BD] \quad (3.6)$$

$$r_{MG} = k_3 [DG][MetOH] - k_4 [MG][BD] - k_5 [MG][MetOH] + k_6 [BD][GL] \quad (3.7)$$

$$r_{GL} = k_5 [MG][MetOH] - k_6 [BD][GL] \quad (3.8)$$

$$r_{MetOH} = -k_1 [TG][MetOH] + k_2 [DG][BD] - k_3 [DG][MetOH] + k_4 [MG][BD] \\ - k_5 [MG][MetOH] + k_6 [BD][GL]$$

$$(3.9)$$

3.3. Physical and Thermodynamics Properties

Thermodynamics properties and equations play a major role in separation operation.

3.3.1. Thermodynamics Properties

Vapor pressure

The vapor pressure of a pure liquid species is well represented over a wide range of temperature (up to critical temperature) by Antoine equation in Pascal [Pa], P^* , from the temperature in kelvin:

$$P^* = \exp \left(A + \frac{B}{T} + C \cdot \ln(T) + D \cdot T^E \right) \quad (3.10)$$

A principal advantage of this equation is that values of the constants A, B, C, D and E are readily available for large number of species in the table 3.2.

Table 3.2. The parameters of vapor pressure [9].

	P^* [Pa]
TG	A=2.347*10 ² B=-3.469*10 ⁴ C=-27.25 D=1.547*10 ⁻¹⁸ E=6
GL	A=99.986 B=-1.3808*10 ⁴ C=-10.088 D=3.5712*10 ⁻¹⁹ E=6
MetOH	A=82.718 B=-6.9045*10 ³ C=-8.8622 D=7.4664*10 ⁻⁶ E=2
BD	A=1.0547*10 ² B=-1.4531*10 ¹⁴ C=-10.98 D=2.5753*10 ⁻¹⁸ E=6

Heat capacity

A common empirical representation of effect of temperature on the ideal gas heat capacity of a pure component is the following third-degree polynomial equation:

$$Cp_l = A + BT + CT^2 + DT^3 + ET^4 \quad (3.11)$$

Where the constants A, B, C, D and E are readily available for each species in the table 3.3.

Table 3.3. Constants for heat capacity

	Cp_l [J/kmol]
TG	A = $9.2969 \cdot 10^5$ B = $2.692 \cdot 10^3$ C = $-4.4542 \cdot 10^{-1}$ D=0 E=0
GL	A= $7.8468 \cdot 10^4$ B= $4.8071 \cdot 10^2$ C=0 D=0 E=0
MetOH	A= $2.5604 \cdot 10^5$ B= $-2.7414 \cdot 10^3$ C = $1.477 \cdot 10$ D= $-3.5078 \cdot 10^{-2}$ E = $3.2719 \cdot 10^{-5}$
BD	A= $2.2999 \cdot 10^5$ B= $9.9221 \cdot 10^2$ C = $6.7574 \cdot 10^{-3}$ D=0 E=0

3.3.3. Physical Properties

Some physical and thermodynamic properties of the compounds involved in the transesterification reaction, essential for modeling are given in Table 3.4. The reported values have been collected from the DIPPR project 801 database [9] as recommended by the American Institute for Chemical Engineers (AIChE), except for the values for monolinoleate [20] and dilinoleate [21] which are not covered in the DIPPR 801 database at the present.

Table 3.4: Physical and thermodynamic properties of the biodiesel compounds [9], [21], [20].

Compound	M _w [kg/kmol]	T _b [K]	T _c [K]	P _c [Pa]	Chemical formula
Trilinoleate(TG)	879.384	895.3	934.6	2.0004	C ₅₇ H ₉₈ O ₆
Dilinoleate (DG)	616.9542	942.6	-	-	C ₃₉ H ₆₈ O ₅
Monolinoleate(MG)	354.524	758.2	-	-	C ₂₁ H ₃₈ O ₄
Glycerol (GL)	92.09	561	850	12.889	C ₃ H ₈ O ₃
Methanol (MetOH)	32.04186	337.85	512.5	79.781	CH ₄ O
Methyl linoleate (BD)	294.472	619.15	767.4	-	C ₁₉ H ₃₄ O ₂

The other properties are the heat of vaporization (ΔH_{vap}) and the density (ρ_l) are also necessary for modeling. These properties are temperature- dependent and are described by equations 3.12-3.13.

$$\rho_l = A/B^{[1+(1-\frac{T}{c})^D]} \quad (3.12)$$

$$\Delta H_{vap} = A(1 - T_r)^{B+CT_r+DT_r^2+ET_r^3} \quad (3.13)$$

In equation 3.14 one can see that the heat of vaporization depends on the reduced temperature, which is defined below in equation 3.15:

$$T_r = \frac{T}{T_c} \quad (3.14)$$

The parameters for these equations are also given in table 3.3. Table 3.3 only contains data for MetOH, TG, BD and GL [9], while temperature- dependent data for DG and MG are presented in the next section.

Table 3.5. Temperature Dependant properties of TG, GL, MetOH and BD [9].

	ΔH_{vap}	ρ_l [kmol/m ³]
TG	A=2.8206*10 ⁸ B=5.2602*10 ⁻¹ C =5.853*10 ⁻¹ D=-7.728*10 ⁻¹	A=2.6085*10 ⁻² B=1.4259*10 ⁻¹ C =9.346*10 ² D=2.857*10 ⁻¹
GL	A=1.1067*10 ⁸ B=4.8319*10 ⁻¹	A=9.2382*10 ⁻¹ B=2.4386*10 ⁻¹ C =8.5*10 ² D= 2.2114*10 ⁻¹
MetOH	A=5.0451*10 ⁷ B=3.3594*10 ⁻¹	A=2.3267 B=2.7073*10 ⁻¹ C =5.125*10 ² D= 2.4713*10 ⁻¹
BD	A=1.2934*10 ⁸ B=9.5883*10 ⁻¹ C=-8.7844*10 ⁻¹ D= 2.8268*10 ⁻¹	A=2.0469*10 ⁻¹ B=2.3737*10 ⁻¹ C =7.674*10 ² D= 2.8571*10 ⁻¹

Estimations for DG and MG

The vapour pressure and liquid density equations for DG and MG had to be estimated, as they were not described in any available database.

The vapour pressure estimations applied Reidels method which is based on the critical temperatures and pressures of the compound. The estimation method applies to the same equation as for the DIPPR 801-derived parameters [22].

The critical temperatures and pressures for MG and DG also had to be estimated. Various methods are available for this purpose with varying degrees of validity and difficulty. For this project, the Joback method was chosen. The critical temperatures and pressures calculated are given in Table 3.6, along with the calculated parameters of the vapour pressure equation. More information along with detailed calculations on the Joback method and the Reidel method is available in Appendix.

Because of the large uncertainties associated with parameter estimations by group contribution methods, the liquid density-equations estimation for DG and MG took a simpler approach; and were estimated as intermediate values of the densities of TG and BD. These equations are also shown in Table 3.6.

Table 3.6: Temperature dependent properties for DG and MG

	T _c [K]	P _c [MPa]	P* [Pa]	ρ _l [kmol/m ³]
DG	1327.79	0.46368	A=-15.931 B=-2111 C =2.4303 D=8.0567*10 ⁻²¹ E = 6	$2/3(\rho_l[TG]) + 1/3(\rho_l[BD])$
MG	932.43	1.1625	A=118.95 B=-20181 C =-14.318 D=9.1481*10 ⁻¹⁹ E = 6	$1/3 \rho_l[TG] + 2/3 \rho_l[BD]$

3.4. Vapor- Liquid Equilibrium

Vapor –liquid equilibrium (VLE) refers to systems in which a single liquid Phase is in equilibrium with its vapor. Analysis of separation equipment usually involves the assumption of phase equilibria as expressed in terms of Gibbs free energy. Chemical potentials, fugacity or activities, usually chemical potential (partial Gibbs free energy) cannot be expressed as an absolutely quantity, and the numerical values of chemical potential are difficult to relate to more easily understood physical quantities. Therefore, fugacity and activity are employed as a substitute to chemical potential [8].

An equilibrium ratio is the ratio of mole fractions of a species present in two phases at equilibrium. For vapor-liquid case, the constant is referred to as K-value or vapor-liquid ratio. A summary of useful formulations for estimating K-values for vapor- liquid equilibrium is shown in table 3.7 below.

Table 3.7. Useful expressions for estimating K-values for vapor-liquid equilibria [18].

		Equations	Recommended application
Rigorous			
1	Equation of state	$K_i = \frac{\bar{\phi}_{iL}}{\bar{\phi}_{iV}}$	Hydrocarbon and light gas mixtures from cryogenic temperatures to the critical region
2	Activity coefficient	$K_i = \frac{\gamma_{iL}\bar{\phi}_{iL}}{\bar{\phi}_{iV}}$	All mixtures from ambient to near critical temperature
Approximate forms:			
3	Rout's law (ideal)	$K_i = \frac{P_i^0}{P}$	Ideal solutions at near-ambient pressure
4	Modified Rout's law	$K_i = \gamma_{iL} \frac{P_i^0}{P}$	Nonideal liquid solutions at near ambient pressure
5	Poynting Correction	$K_i = \gamma_{iL} \bar{\phi}_{iV}^0 \left(\frac{P_i^0}{P}\right) \exp\left(\frac{1}{RT} \int_{P_i^0}^P v_{iL} dP\right)$	Nonideal liquid solutions at moderate pressure and below the critical temperature
6	Henry's law	$K_i = \frac{H_i}{P}$	Low-to-moderate pressures for species at supercritical temperature

Raoult's law is an ideal law that describes vapor- liquid phase behavior at equilibrium. The law is cited in equation (3.15) and equation (3.16) which gives relations for the vapor (y_i) and liquid (x_i) compositions in regard to the vapor pressure (P_i^*) exerted by the liquid in a binary mixture [16].

$$P = x_i P_i^* + x_j P_j^* \quad (3.15)$$

$$y_i = \frac{x_i P_i^*}{p} \quad (3.16)$$

Equation 3.16 can easily be extended to cover multiple component mixtures. However it is common to simplify calculations by introducing a general parameter such as the relative volatility. The relative volatility is a measure for how volatile the compounds are compared to a reference compound. The equations are shown below for a reference compound c [25]:

$$\alpha_i = \frac{y_i/x_c}{y_c/x_c} \quad (3.17)$$

$$y_i = \frac{\alpha_i x_i}{\sum_i \alpha_i x_i} \quad (3.18)$$

A very rough estimation of the relative volatilities for the process was performed by considering the respective boiling points of the compounds, with methanol as the reference compound:

Table 3.8. The values of relative volatilities of TG, DG, MG, GL and BD with respect to Methanol.

α_{MetOH}	α_{TG}	α_{DG}	α_{MG}	α_{GL}	α_{BD}
1	0.01	0.01	0.02	0.05	0.03

However, these correlations are only valid for ideal systems such as benzene-toluene. Even for ideal systems, the relative volatility will change with varying temperatures, and for non-ideal systems they may also change with composition [24].

To correct for non-ideality a parameter called the liquid phase activity coefficient is introduced, which has to do with how the compounds behave towards each other in the liquid phase and whether the combined vapor pressure will be higher or lower than the ideal [25]. The liquid phase activity coefficient can be estimated by application of thermodynamic methods such as UNIFAC/UNIQUAC. These methods are extensive and time consuming and because of time constraints, this method was not implemented in the dynamic model. The vapor phase equation with is shown in equation 3.19 below for low pressure systems [26]:

$$y_i p = \gamma_i x_i P_i^* \quad (3.19)$$

3.5. Enthalpy

Stage Liquid and Vapor Enthalpies

The vapor and liquid enthalpies in each stage is given by the sum of molar enthalpy of component i in stage j and the component flow rates.

$$H_{Lj} = \sum_{i=1}^n h_{Lj} l_{i,j} \quad (3.20)$$

and

$$H_{Vj} = \sum_{i=1}^n h_{Vj} v_{i,j} \quad (3.21)$$

The component flow rates in liquid and vapor phases are expressed as

$$l_{i,j} = L_j X_{i,j} \quad \text{and} \quad v_{i,j} = V_j Y_{i,j} \quad (3.22)$$

The molar enthalpy of component i is expressed as [14]

$$h_{Lj} h_{Vj} = H_{fi}(T_r) + \int_{T_r}^T c_{p_i} dT \quad (3.23)$$

The heat of formation $H_{fi}(T_r)$ for species is presented in below table.

Table 3.9. : Molar heat of formation of component.

Species	ΔH_f [kJ/mol]
TG	-1748
DG	0
MG	0
GL	-669.6
MetOH	-239.1
BD	-605.1

Enthalpies of distillate and bottoms and feed (H_D, H_B, H_F) are estimated from the expressions

$$\mathbf{H}_D = \sum_{i=1}^n \mathbf{h}_{Li,D} \mathbf{D}X_{i,D} \quad (3.24)$$

$$\mathbf{H}_B = \sum_{i=1}^n \mathbf{h}_{Li,B} \mathbf{B}X_{i,B} \quad (3.25)$$

$$\mathbf{H}_F = \sum_{i=1}^n \mathbf{h}_{Li,F} \mathbf{F}X_{i,F} \quad (3.26)$$

4. MATHEMATICAL MODEL DEVELOPMENT

4.1. Introduction

Reactive distillation is being used in industrial applications with more frequency because of increasing research and development of this technology, a result of commercial and academic experience and success.

Despite these recent advances in reactive distillation, there is no generally accepted method for design of distillation with reaction. Most of the systematic methods available possess limitations because of their simplified assumptions. Moreover, these methods have rarely been proven with a variety of reactive distillation processes and they do not consider the design in detail.

A reactive distillation problem has to be studied using different approaches includes: feasibility, simulation, modeling, design and experimental studies in laboratory and the pilot plant. A combination of all of these methods gives rise to the most accurate solution to the problem. One very important aspect of predicting the behavior in these systems is the model that is used to design and simulate the reactive distillation process. In the literature, the most common model that has been used is the equilibrium stage model. The equilibrium stage model is based on the conventional equilibrium-stage model of a distillation column with the addition of the reaction terms in the mass and energy balances.

This chapter describes the detailed derivation and development of mathematical model for equilibrium model of reactive distillation column.

4.2. Modeling of Reactive Distillation

In reactive distillation the quality of the model developed offers a good way to process intensification and the quality and reliability of the calculated results. An effective way of decomposing the modeling aspects of reactive distillation involves the following classification of the model existing for distillation with reaction.

1. Steady state equilibrium stage model
2. Dynamic equilibrium stage model

3. Steady state non-equilibrium stage model
4. Dynamic non-equilibrium stage model

For the purpose of this study, the primary approaches available in the literature for modeling of reactive distillation columns will be the equilibrium stage model.

4.2.1. Equilibrium Stage Model

The development and application of the equilibrium model stage model for conventional distillation has been described in several textbooks. Here, it is focused on the extension of this standard model to distillation accompanied by chemical reactions.

A diagram of an equilibrium stage is shown in figure (4.1b). Vapor from the stage below and liquid from the stage above are brought into contact on the stage together with any fresh or recycle feeds. The vapor and liquid streams leaving the stage are assumed to be in equilibrium with each other. A complete separation process is modeled as a sequence of n of these equilibrium stages (figure 4.1a).

The equilibrium stage model assumes that the vapor and liquid streams leaving a given stage are in thermodynamic equilibrium with one another. These models can be coupled with the assumption of chemical equilibrium at each stage.

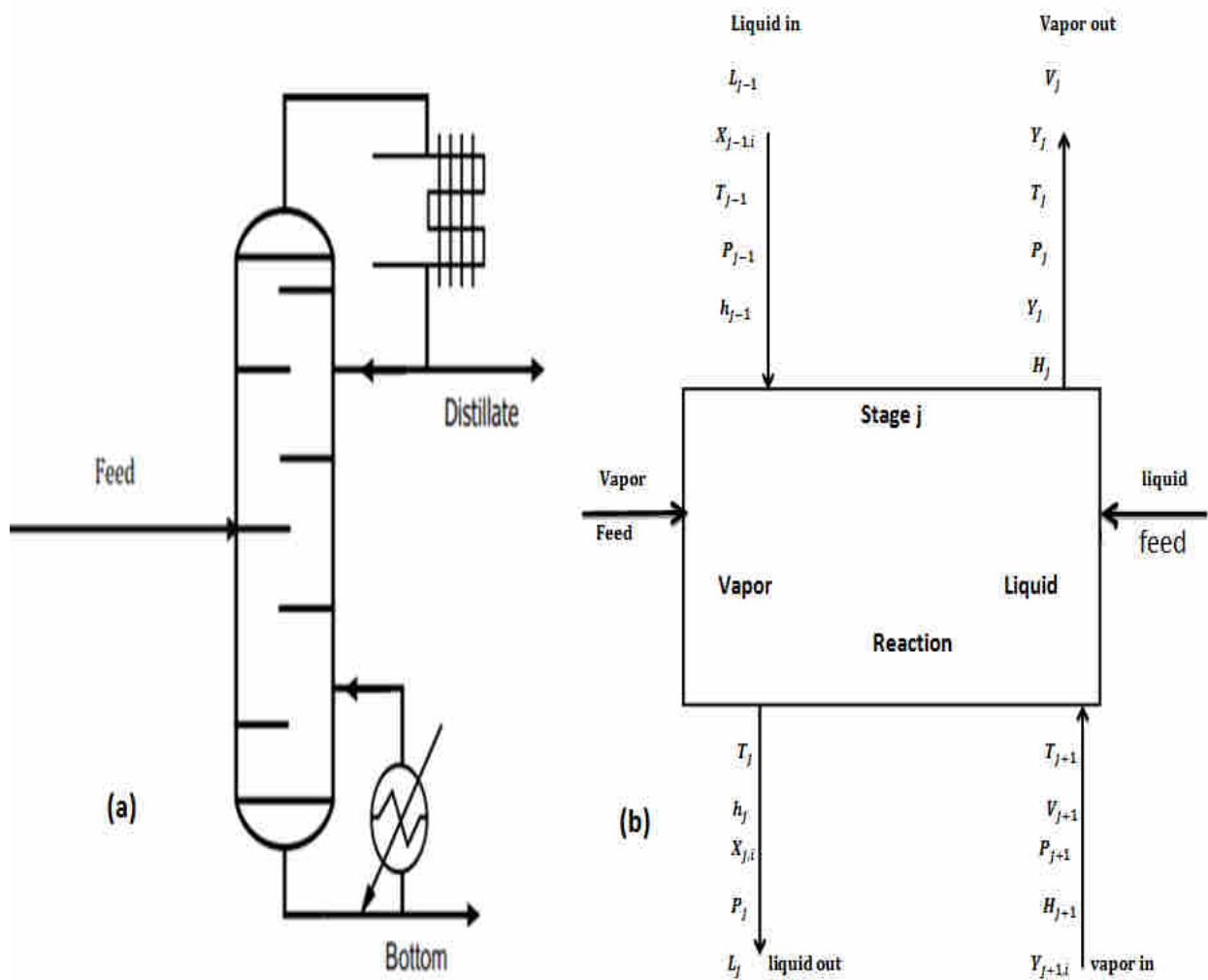


Figure 4.1. (a) Multi-stage distillation column. (b) The equilibrium stage.

Stages are conventionally counted top down at modeling (in contrast to the industrial practice where they are counted bottom up). Pressure of stage j is P_j , its temperature is T_j , molar flow rate of liquid flowing from stage is L_j , its mole fraction is x_j , the molar flow rate of vapor phase is V_j , its mole fraction is y_j . Molar enthalpy of the down flowing liquid is h_j , that of the emerging phase is H_j . From stage $j-1$ above flows down a stream with flow rate L_{j-1} to stage j , and from stage $j+1$ below emerges V_{j+1} , characterized with the respective compositions and molar enthalpies.

Feed flow rate F_j , composition z_j , and some molar enthalpy H_f , may arrive to feed stage. Heat can be introduced to any stage j as Q_j . (Negative Q_j means cooling).

If there are C components in the process then any stage is described by $3C + 9$ scalar variables.

The steady state model consists of 4 main equation groups, the so called MESH equations, and additional auxiliary equation groups.

M: Material balance equations for each component and total balance

E: Equilibrium equations

S: Summation equations or composition constraints

H: Heat balance equations

The liquid and vapor streams leaving each stage are assumed to be equilibrium.

The model equation for a general stage j and component i are represented based on the commonly used distillation equation with the reaction terms.

Total material balance on stage j is

Accumulation = Input - output + rate of generation - rate of consumption

$$\frac{dM_j}{dt} = F_j + V_{j+1} + L_{j-1} - (S_j^v + V_j) - (S_j^l + L_j) + \sum_{m=1}^r \sum_{i=1}^c v_{i,m} R_{m,j} \epsilon_j \quad (4.1)$$

M_j is the hold up of the liquid phase on the stage. The vapor hold up will be neglected.

$\sum_{m=1}^r \sum_{i=1}^c v_{i,m} R_{m,j} \epsilon_j$ is the rate of disappearance of the total moles to any reaction k on stage j .

$v_{i,m}$ - is the stoichiometric coefficient of component i in reaction m .

$R_{m,j}$ - is rate on reaction m in stage j .

ϵ_j - is reaction volume.

The component i material balance on stage j is given below:

$$\frac{d(M_j x_{i,j})}{dt} = F_j Z_{j,i} + V_{j+1} y_{j+1,i} + L_{j-1} x_{j-1,i} - (S_j^v + V_j) y_{i,j} - (S_j^l + L_j) x_{i,j} + \sum_{m=1}^r \sum_{i=1}^c v_{i,m} R_{m,j} \epsilon_j \quad (4.2)$$

The summation equations are:

$$\sum_{i=1}^c x_{j,i} = 1 \text{ and } \sum_{i=1}^c y_{j,i} = 1 \quad (4.3)$$

The phase equilibrium relations

$$y_{j,i} = K_{j,i} x_{j,i} \quad (4.4)$$

The heat balance equations or enthalpy equations are:

$$\frac{d(M_j H_j)}{dt} = F_j H_j^F + L_{j-1} h_{j-1} + V_{j+1} H_{j+1} - (S_j^v + V_j) H_j - (S_j^l + L_j) h_j + Q_j \quad (4.5)$$

The H and h are enthalpies of the appropriate phase (vapor and liquid). The enthalpy in the time derivative on the left hand side represents the total accumulation of enthalpy of the stage but, for the reasons given above; this will normally be liquid-phase enthalpy.

The Murphee efficiency (E_{MV}) can be incorporated into the MESH equations by replacing the equilibrium equations by replacing the equilibrium equation with the definition (Equation 5).

$$(E_{MV})_{j,i} = \frac{(Y_{j,i} - Y_{j+1,i})}{(Y_{j,i}^* - Y_{j+1,i})} \quad (4.6)$$

The concept of efficiency works very well for binary systems. However, for multi-component systems in reactive distillation the values of the efficiencies are uncertain due to the effect of separation coupled with chemical reaction.

4.3. Solution Method

4.3.1. Initial Condition

The initial conditions applied for the models are summarized in Table 4.1

Table 4.1. Initial conditions for the reactive distillation of biodiesel from Simasatitkul et al.[1].

Condition	Value	Comment
Temperature of feed	323.15K	
Pressure	1atm	The pressure drop was considered negligible
Reflux ratio	3	
Duty of reboiler	1.2×10^7 kJ/h	
Number of tray	20	This excludes the reboiler and condenser.
Feed tray	1	The feed is introduced at the first tray (counted from the top) because the feed contains a mixture of methanol and the catalyst. If the feed was to be introduced at a lower point in the column the number of reactive stage would be reduced as no catalyst would be present.
Catalyst	NaOH	NaOH was chosen as the catalyst because of the availability of kinetic data.

The assumptions were made to ease the model simulation:

1. The soybean oil only consists of linoleic esters
2. The pressure drop in the column is considered negligible
3. The rate of saponification and hydrolysis reactions are considered negligible

4. The course of the reaction is completely described by their kinetic equation
5. The mass of the homogenous catalyst is negligible
6. The catalyst will have no effect on the phase equilibrium
7. The reaction will occur in the liquid phase
8. Phase equilibrium is established on every tray
9. The reaction will only occur on actual trays and not in the reboiler or in the condenser.
10. The efficiency of the trays is 100%
11. The vapor behaves as an ideal gas

4.3.2. Initial Estimation

Any solution method is used; unknowns must be estimated before starting iteration. The simplest estimations are listed below.

Equilibrium ratios Equilibrium ratios may be considered as functions of temperature only. One may start up from constant relative volatilities as well.

Composition Expected mole fractions in the products are usually known. Compositions on feed stages are near the feed composition. A linear profile in stage numbers can be applied. Vapor composition can be obtained in simple way with supposed constant relative volatility:

$$y_{i,j} = \frac{x_{i,j} \alpha_i}{\sum_{k=1}^c x_{k,j} \alpha_k} \quad (4.7)$$

Internal flow rate usual design variables are distillate flow rate (D) and reflux ratio(R); hence flow rates in the top of the column can be determined:

$$L_1 = RD \quad (4.8)$$

$$V_1 = (R+1) D \quad (4.9)$$

The other flow rate along the column can be calculated with material balance and constant molar overflow approximation:

$$L_j = L_{j-1} + q_j F_j \quad (j = 2, \dots, N) \quad (4.10)$$

$$V_{j+1} = L_j + V_j - L_{j-1} - F_j \quad (j = 1, \dots, N) \quad (4.11)$$

Where q_j is estimated liquid phase ratio of the feed to stage j .

4.3.3. Computational Algorithms for Reactive Distillation

Computational methods used to solve the simultaneous chemical reaction and vapor- liquid equilibrium equations are extensions to the algorithms for solving conventional distillation methods.

Based on pure distillation methods, a similar classification is adopted for computational methods with reaction and distillation. The methods include;

- Equation tearing methods
- Relaxation methods
- Newton – based method
- Inside- out methods
- Hemotopy- continuation methods

Inside- out, Hemotopy- continuation and relaxation methods are extension of the equation tearing and newton – based method. The usefulness of these methods are limited by simplification, assumption made and the number of and type of reactive distillation systems they have been used to simulate. Attempts to solve the reactive distillation problems more accurately and efficiently have led to a variety of methods that combine the advantages of different methods. The most successful methods are listed below.

1. Equation tearing or sequential method

These methods involve the partitioning of MESH equations, allowing them to be solved separately in a series of steps. Sequential or tearing method includes bubble –point methods (BP) and sum-rate methods (SR) methods. These algorithms are fast and efficient.

2. Inside –out method

The inside –out method is a very robust algorithm that can solve a wide variety of problems. These methods generate parameters for each stage, which are used for simple k-value and enthalpy models (i.e. equilibrium ratio and energy balance).

In general, these procedures make use of equation partitioning in conjunction with equation tearing and linearized Newton-rahpson techniques. In present study equation-tearing or sequential procedure using tri-diagonal- matrix algorithm is used to solve the equilibrium model equations.

3. Hemotopy- continuation methods

Homotopy – continuation methods are employed most often for solving problems that are considered very difficult to solve with other methods. Although the simultaneous correction and inside-out methods are reasonably robust, they are not guaranteed to converge and sometimes fail, particularly for every non-ideal liquid solution and when initial guesses are poor. A much more robust, but more time- consuming, method is differential arc length homotopy continuation.

In the present study equation-tearing procedure using the Tri-diagonal-matrix Algorithm is used to solve the equilibrium model equations.

4.3.4. Equation – Tearing or Sequential Procedures

Friday and smith (1964) systematically analyzed a number of tearing techniques for solving the MESH equations. They carefully considered the choice of output variable for each equation.

Tearing methods are assigning tearing variables and these are updated in iteration cycles. Other variables can be computed in well-defined calculation sequences as functions of actual values of tearing variables.

In general the modern equation- tearing procedures are readily programmed, are rapid, and required a minimum of computer storage. More powerful, flexible, and reliable computer programs are based on the application of sparse matrix methods for solving simultaneously all or at least some of the equations.

The Tri-diagonal- Matrix Algorithm

The key to success of these tearing procedures is the tri-diagonal matrix that results from a modified form of the mass balance equations when they are torn from the other equations by selecting T_j and V_j as tearing variables, which leaves the modified M- equation linear in the unknown liquid mole fractions.

These equations have a special form because at most three stage index values takes place in each equation (i.e. the stage to which the balance is made (j), the next upper stage (j+1), and the next lower stage(j-1)). Thus coefficient of matrix is of a tri-diagonal one. These set of equations for each component is solved by a highly efficient and reliable modified Gaussian elimination algorithm. The tri-diagonal matrix is obtained by rearranging MESH equation as follow:

The steady state component material balance is

$$F_j Z_{j,i} + V_{j+1} Y_{j+1,i} + L_{j-1} X_{j-1,i} - V_j Y_{i,j} - L_j X_{i,j} - \Delta R_{j,i} = 0 \quad (4.12)$$

Where $\Delta R_{j,i}$ is the rate of consumption of component i in stage j.

Phase equilibrium equation for each component is:

$$Y_{j,i} = K_{j,i} X_{j,i} \quad (4.13)$$

Substituting equation 4.13 into equation 4.12 to eliminate Y:

$$F_j Z_{j,i} + (V_{j+1} K_{j+1,i}) X_{j+1,i} + L_{j-1} X_{j-1,i} - (V_j K_{j,i}) X_{j,i} - L_j X_{i,j} - \Delta R_{j,i} = 0 \quad (4.14)$$

Summation equation

$$\sum_{i=1}^c \mathbf{x}_{j,i} - \mathbf{1} = \mathbf{0} \quad (4.15)$$

$$\sum_{i=1}^c \mathbf{y}_{j,i} - \mathbf{1} = \mathbf{0} \quad (4.16)$$

Energy balance equation for each component is given as:

$$\mathbf{F}_j \mathbf{H}_j^F + \mathbf{L}_{j-1} \mathbf{h}_{j-1} + \mathbf{V}_{j+1} \mathbf{H}_{j+1} - \mathbf{V}_j \mathbf{H}_j - \mathbf{L}_j \mathbf{h}_j + \mathbf{Q}_j = \mathbf{0} \quad (4.17)$$

A total material balance equation is derived by combining these two equations and $\sum_{i=1}^c \mathbf{Z}_{j,i} = \mathbf{1}$ with equation 4.12 summed over the C component and over stages 1 through j to give:

$$\mathbf{L}_j = \mathbf{V}_{j+1} + \sum_{m=1}^j (\mathbf{F}_m - \mathbf{dR}_m) - \mathbf{V}_1 \quad (4.18)$$

Where \mathbf{dR}_m is total consumption of components in stage m.

Substituting equation 4.18 into equation 4.14 to eliminate L:

$$\mathbf{F}_j \mathbf{Z}_{j,i} + (\mathbf{V}_{j+1} \mathbf{K}_{j+1,i}) \mathbf{X}_{j+1,i} + (\mathbf{V}_j + \sum_{m=1}^j (\mathbf{F}_m - \mathbf{dR}_m)) \mathbf{X}_{j-1,i} - (\mathbf{V}_j \mathbf{K}_{j,i}) \mathbf{X}_{j,i} - (\mathbf{V}_{j+1} \sum_{m=1}^j (\mathbf{F}_m - \mathbf{dR}_m)) \mathbf{X}_{i,j} - \Delta \mathbf{R}_{j,i} = \mathbf{0} \quad (4.19)$$

After rearranging equation 4.19 we get:

$$\begin{aligned} & \mathbf{F}_j \mathbf{Z}_{j,i} + (\mathbf{V}_j + \sum_{m=1}^j (\mathbf{F}_m - \mathbf{dR}_m)) \mathbf{X}_{j-1,i} \\ & [(\mathbf{V}_{j+1} + \sum_{m=1}^j (\mathbf{F}_m - \mathbf{dR}_m) + \mathbf{V}_j \mathbf{K}_{j,i}) \mathbf{X}_{j,i} + (\mathbf{V}_{j+1} \mathbf{K}_{j+1,i}) \mathbf{X}_{j+1,i} - \Delta \mathbf{R}_{j,i} = \mathbf{0} \end{aligned} \quad (4.20)$$

The equation 4.20 can be expressed as:

$$\mathbf{A}_j \mathbf{x}_{j-1,i} + \mathbf{B}_{j,i} \mathbf{x}_{j,i} + \mathbf{C}_j \mathbf{x}_{j+1,i} = \mathbf{D}_{j,i} \quad (4.21)$$

$$\text{Where } \mathbf{A}_j = \mathbf{V}_j + \sum_{m=1}^{j-1} (\mathbf{F}_m - \mathbf{U}_m - \mathbf{dR}_m)$$

$$\mathbf{B}_{j,i} = \mathbf{V}_{j+1} \mathbf{K}_{j+1,i}$$

$$\mathbf{C}_j = -\mathbf{V}_j \mathbf{K}_{j,i} + \mathbf{V}_{j+1} + \sum_{m=1}^j (\mathbf{F}_m - \mathbf{U}_m - \mathbf{dR}_m) \quad (4.22)$$

$$\mathbf{D}_{j,i} = -\mathbf{F}_j \mathbf{Z}_{j,i} - \Delta \mathbf{R}_{j,i}$$

Properties calculation

$$K_{j,i} = K_{j,i}(T_j, P_j, x_{j,i}, y_{j,i})$$

$$H_j = H_j(T_j, P_j, y_{j,i}) \quad (4.23)$$

$$h_j = h_j(T_j, P_j, x_{j,i})$$

$$\begin{bmatrix} B_1 & C_1 & 0 & \dots & \dots & \dots & 0 & 0 \\ A_1 & B_2 & C_1 & \dots & \dots & \dots & 0 & 0 \\ 0 & A_2 & B_3 & \dots & \dots & \dots & 0 & 0 \\ \vdots & \vdots & \vdots & \dots & \dots & \dots & 0 & 0 \\ \vdots & \vdots & \vdots & \dots & \vdots & \vdots & \vdots & \vdots \\ \dots & \dots & \dots & \dots & \vdots & \vdots & \vdots & \vdots \\ 0 & \dots & \dots & \dots & 0 & A_{N-2} & B_{N-2} & C_{N-1} \\ 0 & \dots & \dots & \dots & 0 & 0 & A_N & B_N \end{bmatrix} \begin{bmatrix} x_{1,i} \\ x_{2,i} \\ x_{3,i} \\ \vdots \\ \vdots \\ \vdots \\ x_{N-1,i} \\ x_{N,i} \end{bmatrix} = \begin{bmatrix} D_1 \\ D_2 \\ D_3 \\ \vdots \\ \vdots \\ \vdots \\ D_{N-1} \\ D_N \end{bmatrix} \quad (4.24)$$

Each set of n equation is a special type of sparse matrix equation called a tri-diagonal-matrix equation. The subscript i has been dropped from the coefficients A, B, C and D in equation 4.24 for convenience. For this type of sparse matrix equation, a highly efficient version of the Gaussian elimination procedure called the Thomas algorithm is applied, which avoids matrix inversion, eliminate the need to store the zero coefficients in the matrix, and also avoids buildup of truncation errors. Furthermore, computed values of $x_{j,i}$ are almost always positive.

4.4. Degree of Freedom Analysis

To examine the number of variables and the number of equations required to solve the model, the difference between the number of variables and number of equations involved in the relationship has been called "Degree of freedom ". A degree of freedom analysis was first developed by Gilliland and Reed ,1942 and modified by Kwauk,1956. If the column consists of N stages and the number of components presented in feed is C, then the column can be defined as shown in table (4-2) as follows:

Table 4.2. Number of variables and equations

Number of variables	
Liquid flow rates	N
Vapor flow rates	N
Liquid composition	C.N
Vapor composition	C.N
Temperature	N
Total	$N(3 + 2C)$
Number of equations	
Total material balance equations	N
Total energy balance equations	N
Component material balance equations	C.N
Equilibrium equations	C.N
Summation equations	N
Total	$N(3 + 2C)$

Since the number of equations is equal to number of variables, then the model can be solved to evaluate:

- ❖ Liquid flow rate in the column.
- ❖ Liquid composition profiles.
- ❖ Vapor composition profiles.
- ❖ Amount of Distillate and Bottom product.
- ❖ Temperature profiles in the column.
- ❖ Vapor flow rate in the column

4.5. Bubble Point Method for Distillation

Frequently, distillation involves species that cover a relatively narrow range of vapor-liquid equilibrium ratio. A particularly effective solution procedure for this case was suggested by Friday and Smith (1964) and developed in detail by Wage and Henke.

It is referred to as bubble point method because a new set of stage temperature is computed during each iteration from bubble point equation.

In the method, all equations are partitioned and solved sequentially except for the modified M-equations, which are solved separately for each component by the tri-diagonal matrix technique.

The algorithm for solving such systems of equations proceeds by the following steps:

1. Specify N and all values of C , $Z_{i,j}$, T_{fj} , P , R , F_j and Q_j .
2. The initial liquid compositions over each tray ($x_{i,j}$) was assumed and normalized.
3. Initial stage temperature was determined from Antoine equation, and from product of initial composition fraction and the calculated saturated temperature.
4. Using specified stage pressure, current estimated stage of temperature and current estimated of stage of vapor and liquid flow rates.
5. Estimate all vapor-liquid equilibrium ratio of each tray ($k_{i,j}$).
6. Computations commenced with $i=1$ and elements of the tri-diagonal matrix A_j , B_j and C_j were then evaluated using all assumed or calculated L_j and V_j .
7. The matrix equation was then solved for $x_{i,j}$ using Thomas algorithm [17], substituting the initial value of $x_{i,j}^0$ as calculated in step 1 for the constant terms of the matrix $D_{i,j}$.
8. Successive substitution according to equation is continued to apply repetitively until convergence in $x_{i,j}$ is obtained. As a test of convergence the following criteria is used

$$\sum_{j=1}^N (x_{i,j}^{k+1} - x_{i,j}^k)^2 \leq \text{Tolerance}$$

9. When convergence was achieved in above step were repeated for all components for $i = 2, 3, 4, 5,$ and 6 . This was done for all the values of $x_{i,j}$ (for $i = 1$ to 6 and $j = 1$ to 20).
10. The values of liquid composition is checked and normalize the value of the liquid composition by

$$x_{i,j}^{normalize} = \frac{x_{i,j}}{\sum_i x_{i,j}} \quad (4.25)$$

to get fastest convergence.

11. Compute a new set of values of T_j tear variables by computing one at time, the bubble point temperature at each stage based on the specified stage pressure and corresponding normalized $x_{i,j}$ values.

$$\sum_i^c k_{i,j} x_{i,j} - 1 = 0; \quad (4.26)$$

12. Calculate values of $y_{i,j}$ one at a time from equation 4.13.
13. Compute vapor and liquid flow rates in each stage across the length of the column were evaluated from the enthalpy data using energy balance equation that is obtained by combining equation 4.17 and equation 4.18, twice to eliminate L_{j-1} and L_j . After rearrange we get:

$$\alpha_j V_j + \beta_j V_{j+1} = Y_j \quad (4.27)$$

$$\text{Where } \alpha_j = h_{j-1} - H_j \quad (4.28)$$

$$\beta_j = H_{j+1} - h_j \quad (4.29)$$

$$Y_j = [\sum_{m=1}^{j-1} (F_m - dR_m)](h_j - h_{j-1}) + F_j(h_j - h_j^F) + Q_j \quad (4.30)$$

and enthalpies are evaluated at the stage temperatures, last computed rather than at those used to initiate the iteration. Written in di-diagonal matrix form equation 4.27 applied over stages 2 to N-1.

$$\begin{bmatrix} \beta_2 & 0 & 0 & \dots & \dots & \dots & 0 & 0 \\ \alpha_3 & \beta_3 & 0 & \dots & \dots & \dots & 0 & 0 \\ 0 & \alpha_4 & \beta_4 & \dots & \dots & \dots & 0 & 0 \\ 0 & 0 & \alpha_4 & \dots & \dots & \dots & 0 & 0 \\ \vdots & \vdots & \vdots & \dots & \vdots & \vdots & \vdots & \vdots \\ \dots & \dots & \dots & \dots & \vdots & \vdots & \vdots & \vdots \\ 0 & \dots & \dots & \dots & 0 & \alpha_{N-2} & \beta_{N-2} & 0 \\ 0 & \dots & \dots & \dots & 0 & 0 & \alpha_{N-1} & \beta_{N-1} \end{bmatrix} \begin{bmatrix} V_3 \\ V_4 \\ V_5 \\ \vdots \\ \vdots \\ \vdots \\ V_{N-1} \\ V_N \end{bmatrix} = \begin{bmatrix} Y_2 - \alpha_2 V_2 \\ Y_3 \\ Y_4 \\ \vdots \\ \vdots \\ Y_{N-1} \\ Y_N \end{bmatrix} \quad (4.31)$$

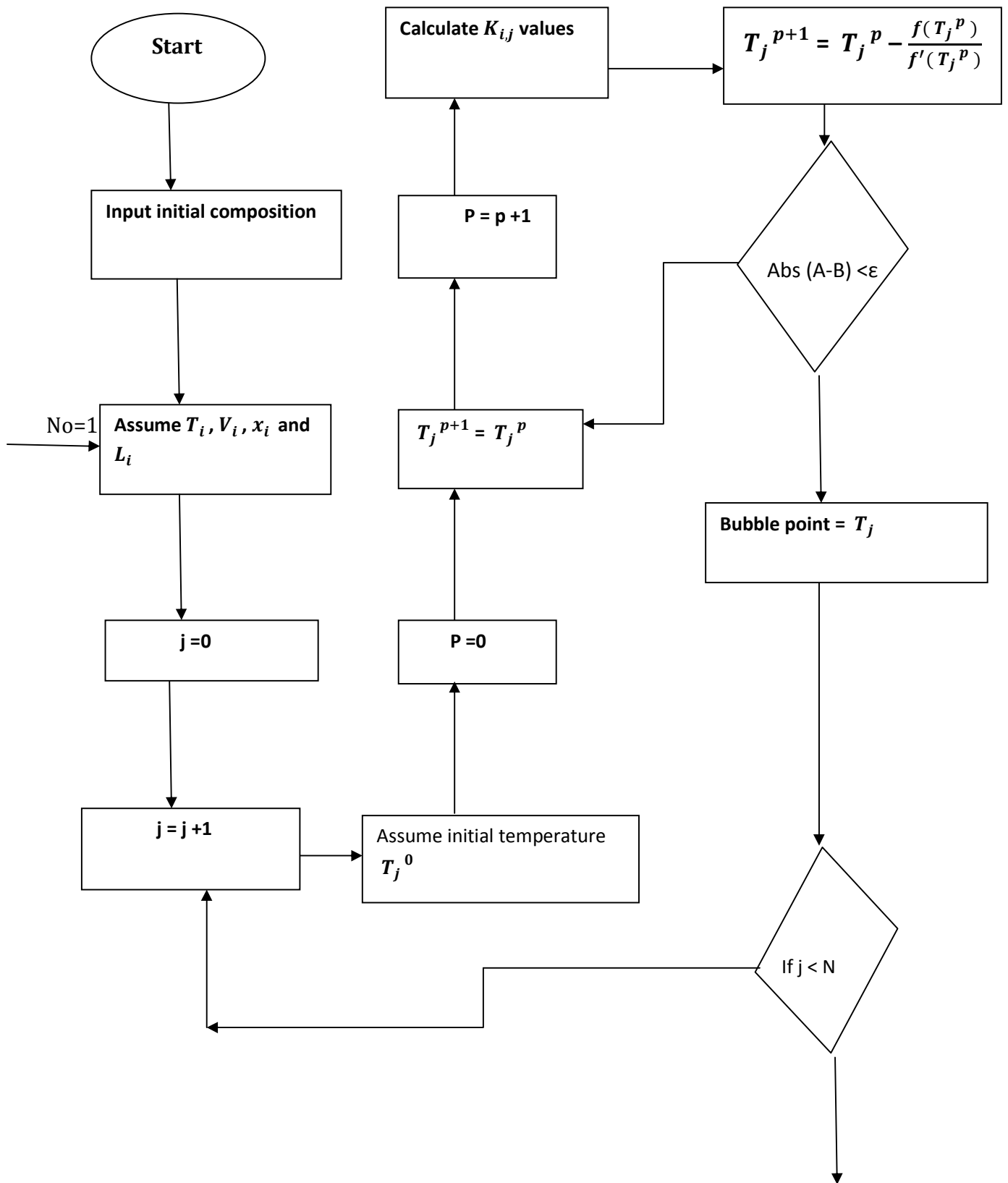
14. The solution procedure is considered to be converged when sets of T_j^k and V_j^k values are within some prescribed tolerance of corresponding sets of T_j^{k+1} and V_j^{k+1} values. One possible convergence criterion is :

$$\sum_{j=1}^N (T_j^{k+1} - T_j^k)^2 \leq \text{Tolerance}$$

where N is the number of stages.

15. The temperature profile and the composition distribution of all the components along the height of the column were obtained after convergence.

The algorithm is summarized below.



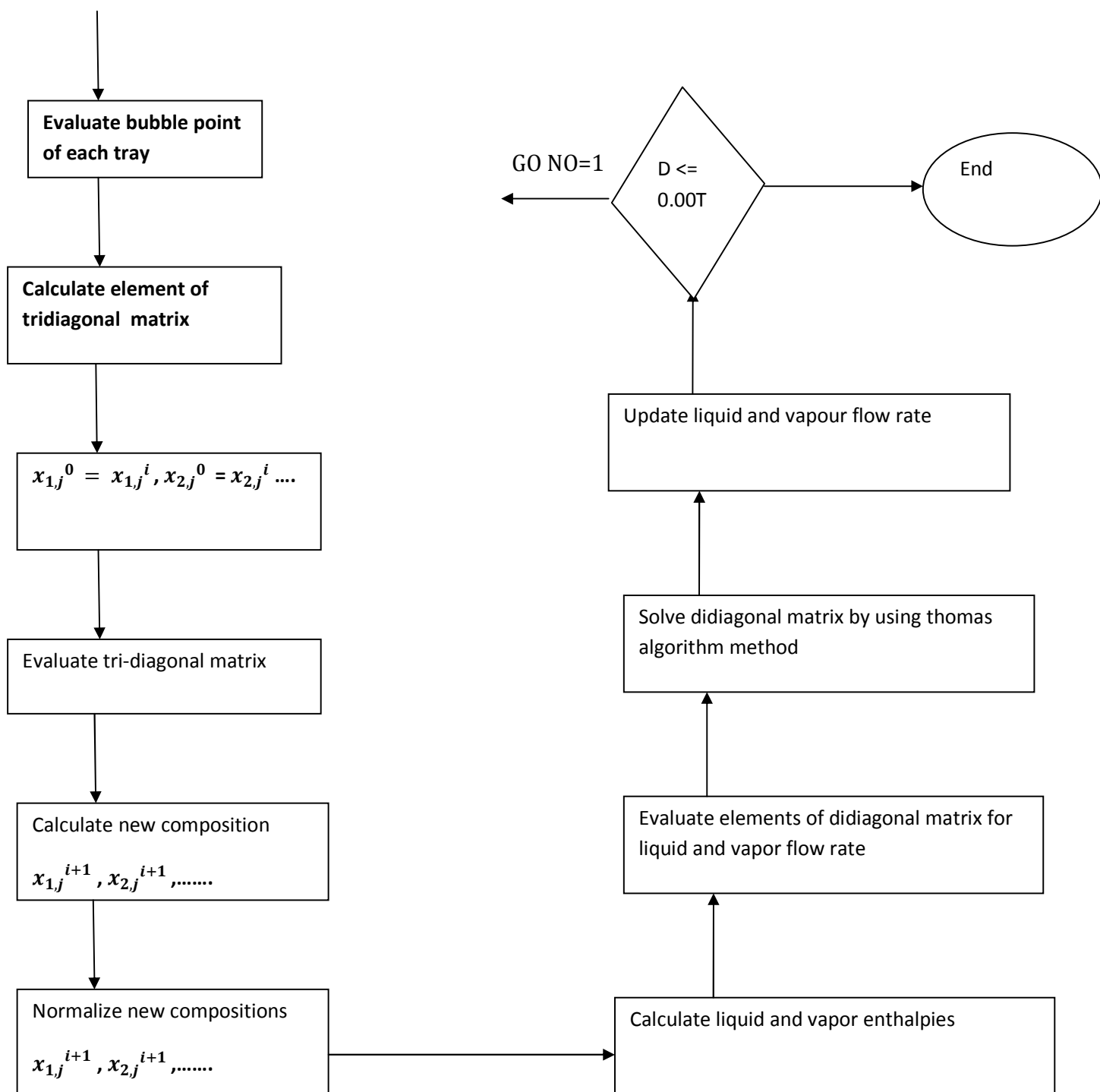


Figure 4.2. Flow Chart of Simulation Program for Continuous Reactive distillation.

Where $A = T_j^{p+1}$

$$B = T_j^p$$

N= specified number of stages

$$D = \sum T_E$$

4.6. Simulation by MATLAB

The design of a distillation column with a simulation program requires a large number of individual computer runs. Different programs have been developed to perform such calculation using different computer languages (Java, FORTRAN, C, C++ ...)

Among all of these programs, MATLAB environment (Version 7) is selected because of its high-level technical computing language and interactive environment for algorithm development, data visualization, data analysis and numerical computation. The MATLAB language supports the vector and matrix operations that are fundamental to engineering and scientific problems (MATLAB web site).

MATLAB provides several types of functions for performing mathematical operations and analyzing data, such as matrix manipulation, linear algebra, polynomials and interpolation, ordinary differential equations, partial differential equations, sparse matrix operations, 2D and 3D plotting and much more.

The program or code is developed for solving equilibrium models of reactive distillation. Equation tearing procedure using tridiagonal matrix algorithm is systematically developed and linked with the sub routine programs necessary to solve the set of equations associated with equilibrium model of the reactive distillation column.

The developed code to simulate the process is described in the appendix section. The simulation result of the equilibrium models of the reactive distillation is discussed in chapter 5.

5. RESULT AND DISCUSSION

5.1. Introduction

The model can be evaluated by the comparison with experimental result or even with different theoretical results that use different simulation or solution method.

The production of biodiesel from triglyceride and methanol by RD is used as a first case to reveal the effects of some variables such as number of feed temperature, reflux ratio and feed ratio. The feed ratio effect is also studied although the 6:1 molar of each of triglyceride and methanol is preferred to avoid separation problems.

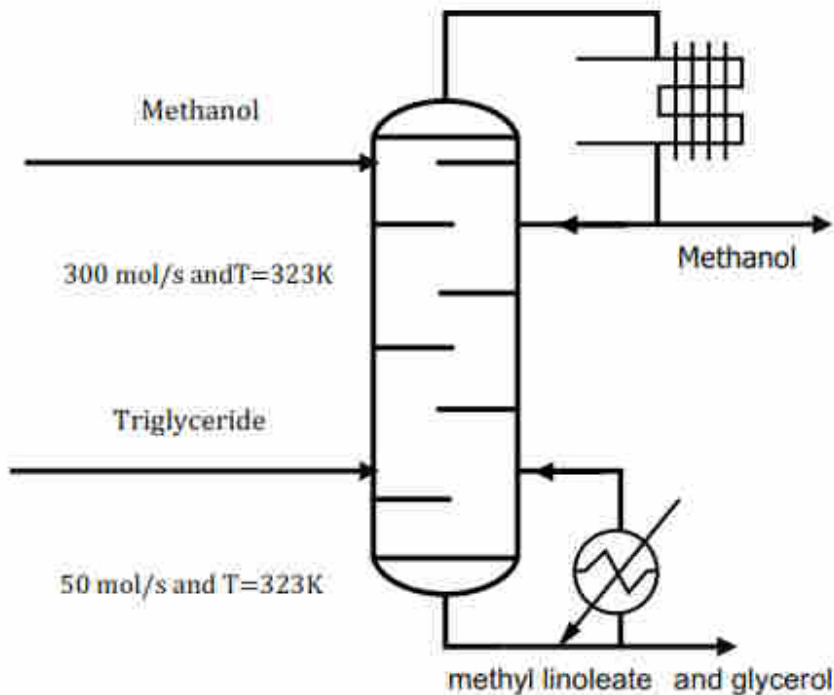


Figure 5.1. A modified flow sheet of the reactive distillation process from Simasatitkul et al.[1]

The conditions that have been applied to the model, that were specified in this report [1], are given in Table 3.1. The total amount of catalyst in the reactive zone is 800kg.

Table 5.1. Operational condition and column specification for the reactive distillation simulation.

Condition and specification	
Feed temperature	323K
Total feed flow rate	350mol/s
Tray type	Sieve
Column diameter	5.595m
Weir length	21.62m
Weir height	0.05m
Downcomer clearance	0.03m
Downcomer area	2.68m ²
Total tray area	24.5m ²

5.2. Validation of Simulation Results

Computer codes developed in the present study using MATLAB program have been validated using the reactive distillation column configuration reported in literature [4]. The simulation results of equilibrium models compared with the simulation result using Raoult's law reported in the literature [4]. It can be seen from figure 5.2 and from table 5.2. the simulation results are comparable with the literature values. The values that resulted from the thesis work and the resulted from Emile's work are comparable but it is slightly different due to initial fresh feed flow rate assumption and the amount of the packing catalyst.

Table 5.2. Comparison between results obtained in this work and those by Emilie Øritsland Houge et.al (2012).

Component	Emilie Øritsland Houge			Equilibrium model simulation result		
	MetOH	GL	BD	MetOH	GL	BD
Tray 1	0.9999	0.0000	0.0000	1.0000	0.0000	0.0000
Tray 10	0.4127	0.0688	0.5504	0.4383	0.0899	0.3361
Tray 20	0.1019	0.0792	0.4906	0.2536	0.2981	0.4159

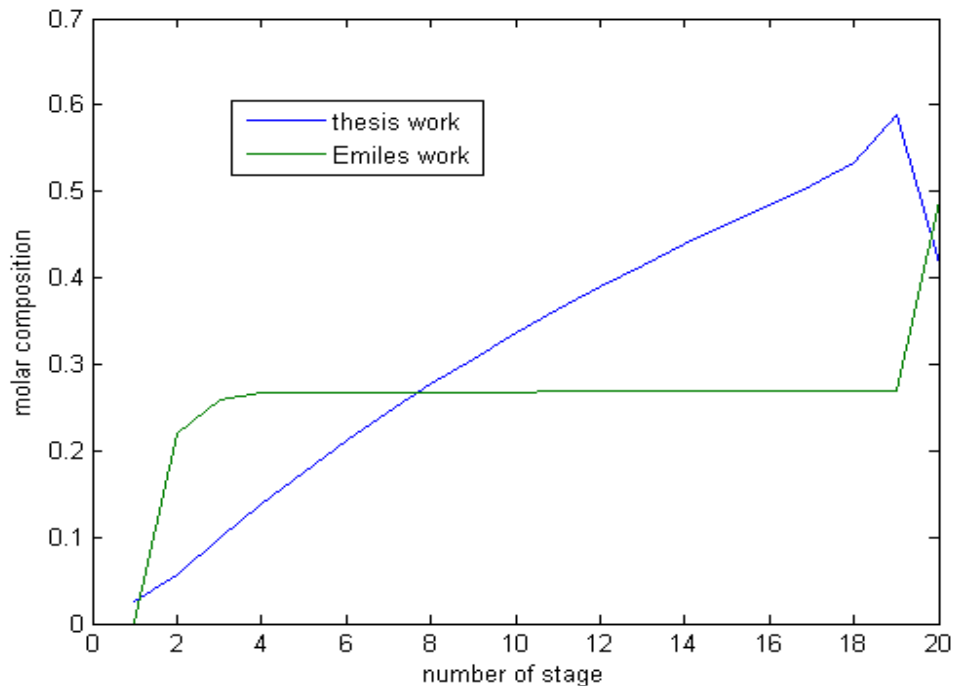


Figure 5.2. The liquid concentration of methyl linoleate under simulation results from thesis work vs results from Emile’s work.

5.3. Simulation of concentration profile

The vapor and liquid phase concentration profiles of the reactive distillation column obtained from equilibrium model simulation results are presented and discussed in this section.

The vapor phase concentration profile expressed in component mole fractions is shown in figure 5.3. The inert component methanol is observed to be the predominant components in the vapor in rectify section. High mole fraction of glycerol and methyl linoleate are achieved at the bottom part of the column. The mole fraction of methyl linoleate and glycerol reach maximum on the bottom of the column. From the bottom stage either end of the reactive distillation column, the mole fraction of methyl linoleate and glycerol decrease, with minimum values in the condenser is greater than that of the remaining component. This is because glycerol is more volatile than methyl linoleate.

In contrast, the mole fraction of biodiesel is opposite to that of methanol. The biodiesel is mostly present in the stripping section; its large mole fraction in the bottoms corresponds to composition of the boil up from the reboiler.

The composition of methanol is decreased as we moved from stage 1 to stage 2 and from stage 19 to stage 20 as the same time the composition of the methyl linoleate and glycerol is steady increased. The figure 5.3. along the internal section of the column the composition of the methanol is the same as the composition methanol at stage 3.

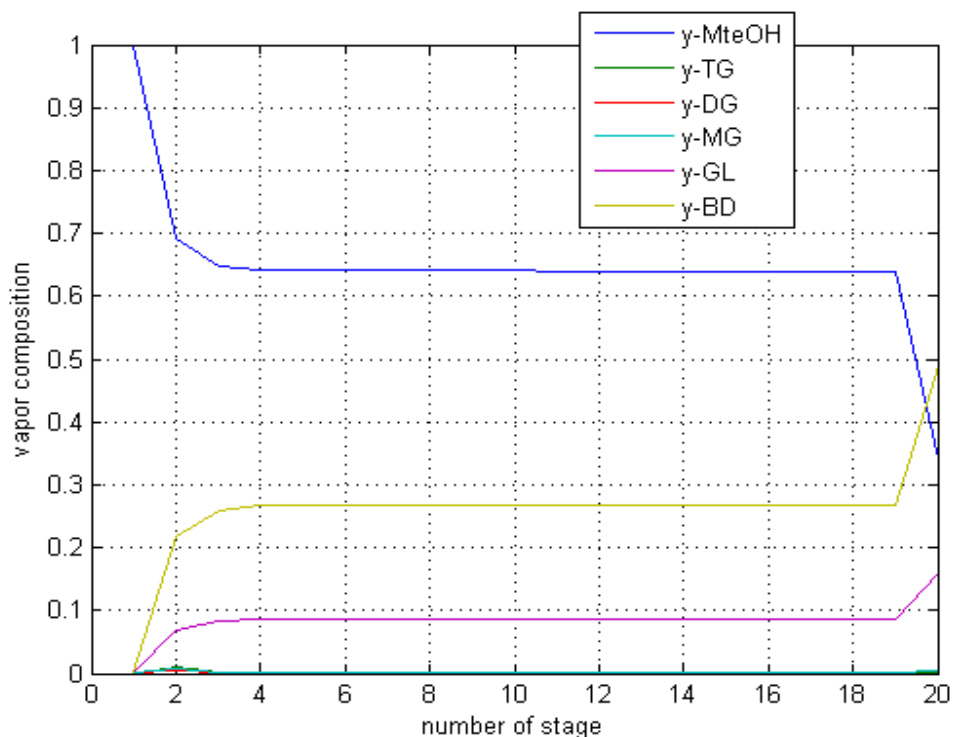


Figure 5.3. Concentration profile for vapor phase using equilibrium model

The liquid phase concentration profile of the component methanol, trillion, diglycide, monoglycide, glycerol and methyl linoleate are shown in Figure 5.4. In the stage 4 to 11 methanol are consumed and as a result, its mole fraction is decreased. Maximum mole fraction of methanol is observed at the feed locations. The liquid composition profile shows that the liquid is dominated by methanol from top stage to down bottom stage, thus

reducing the rate of reaction. In the stripping section, the liquid becomes richer in methyl linoleate.

In rectifying section of the reactive distillation column the concentration of methyl linoleate is low.

In the stripping zone methanol, glycerol and methyl linoleate are being separated, resulting in a high concentration of biodiesel in the bottom. High mole fraction of methyl linoleate is obtained in the liquid phase. This is desirable because methyl linoleate is the product of interest.

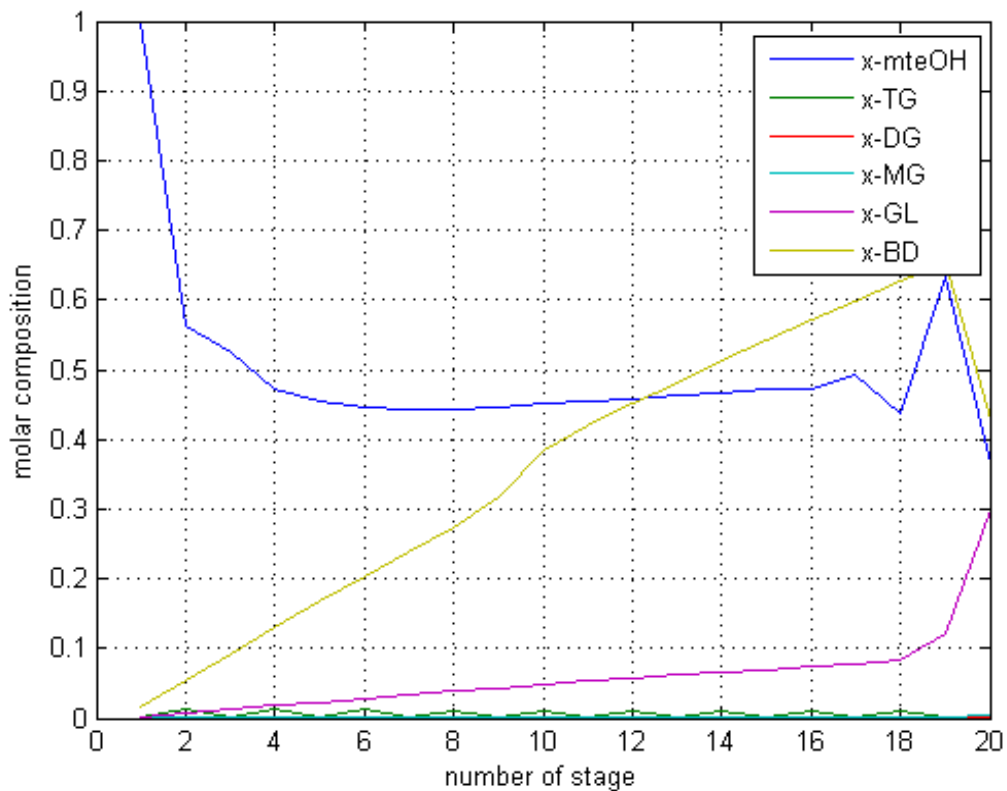


Figure 5.4. Concentration profile for liquid phase using equilibrium model

5.4. Simulation of Temperature Profile

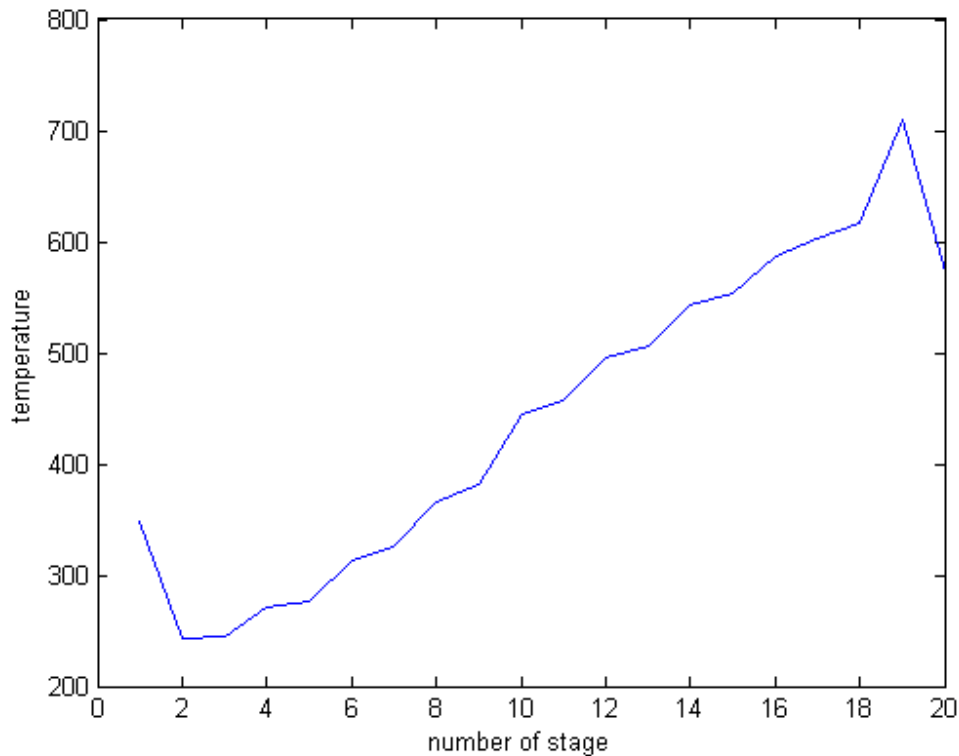


Figure 5.5. Temperature profile for equilibrium model.

The temperature profile of the reactive distillation column obtained from equilibrium model simulation result is shown in Figure 5.5. The profile ranged from 259K (around the condenser) to 730K (around the reboiler). The temperature had a steady rise from stage 2 to stage 19 of the column. The effect of chemical reaction and feed temperature input made the temperature profile to exhibit steady rise from the top to the bottom of the column. At the top of the column (stage 1) the temperature of the column is the same as the temperature of the feed (323K) and it decrease to 259K (temperature at stage 2) due to the effect of incoming condensed reflux temperature and concentration. The peak temperature obtained at stage 19 because of the incoming reboiled reflux. From the figure 5.5 the temperature decrease goes down from stage 19 to stage 20 due to the absence of the reaction and increase of the concentration of methyl linoleate and glycerol.

5.5. Sensitive Analysis

The performance of a process is commonly measured in terms of yield and conversion. The conversion is a measure of how much of limiting reagent is used up in the reaction, while the yield is a measure of how much product is obtained from the limiting reagent. The properties can be calculated by applying equation 5.1 and 5.2 below for the production of methyl linoleate through transesterification reaction of methanol and trillionolien.

$$\text{Conversion} = \frac{F_{0,\text{trilliolien}} - F_{t,\text{trilliolien}}}{F_{0,\text{trilliolien}}} \quad 5.1$$

$$\text{Yield} = \frac{F_{\text{methyl linoleate}}}{F_{0,\text{trilliolien}}} \quad 5.2$$

5.5.1. Effect of Reflux Ratio

The effect of reflux ratio on conversion and yield has been studied simultaneously. The maximum values for both of conversion and yield were when the reflux ratio equal to three Figure (5.4). However, at this reflux ratio, the concentration of the methyl linoleate and glycerol is dominated the the amount of methanol trillion unreacted. As observed from the figure 5.6a and figure 5.6b, as the reflux ratio increase the amount of methanol at the bottom of the distillation as the result the amount of the biodiesel and glycerol decreased as the same time the conversion of the trillion is increased but the amount of the bottom product is decreased. From figure 5.4. the conversion of trillion was smaller than compared to the figure 5.6a and figure 5.6b but the amount of methyl linoleate would be higher than that of reflux ratio 4 and 5. Therefore, to get more products at the bottom of the column the reflux ratio would be 3.

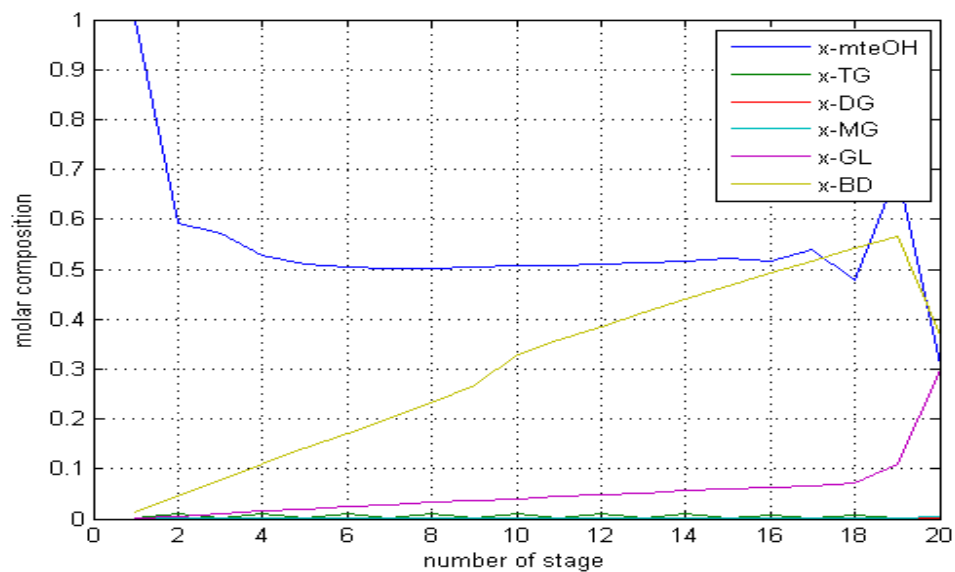


Figure (5.6a) Liquid composition profile with reflux ratio =4

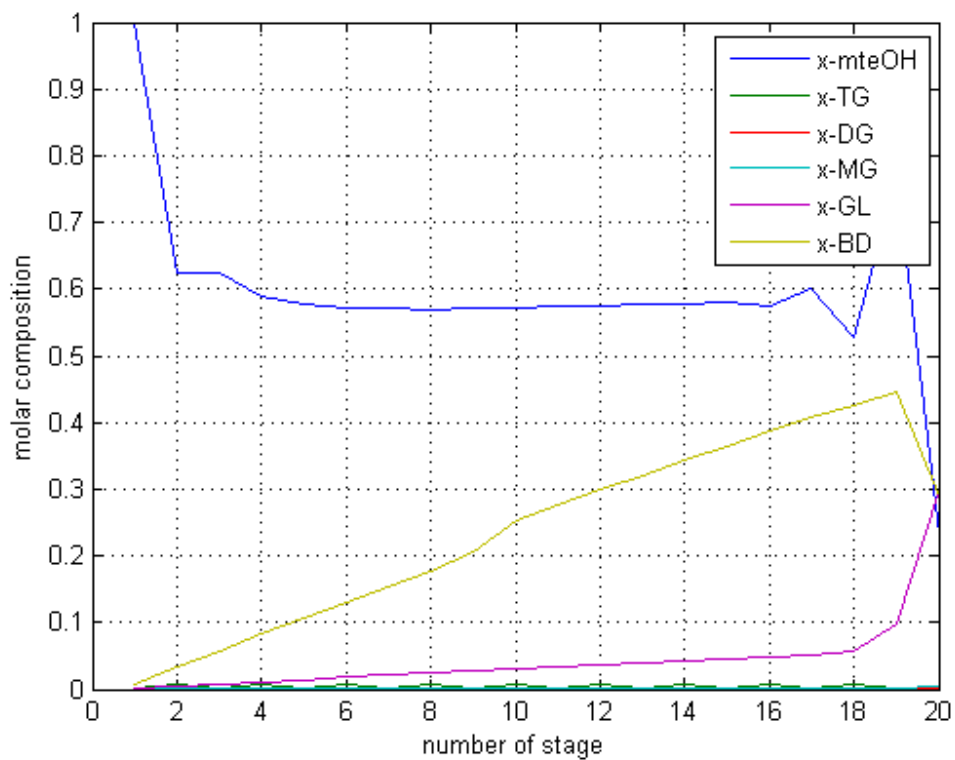


Figure (5.6b) Liquid composition profile with reflux ratio =5.

5.5.2. Effect of Trillion Feed Concentration

A sensitivity analysis is carried out by varying the methanol concentrations in the feed stream of methanol and trillion mixtures and calculating the overall conversion of trillion in the reactive distillation column. As shown in figure 5.7. The conversion of trillion increases as its concentration in the feed stream of methanol and trillion mixture increase. The amount of the feed flow rate is increased then the amount of the trillion in the feed stream is increased as the result the reaction in the column is increased. Thus, the conversion of the trillion is increased as the feed stream flow rate increased. The figure 5.7. shown that the conversion of trillion is dependent on the flow rate feed stream.

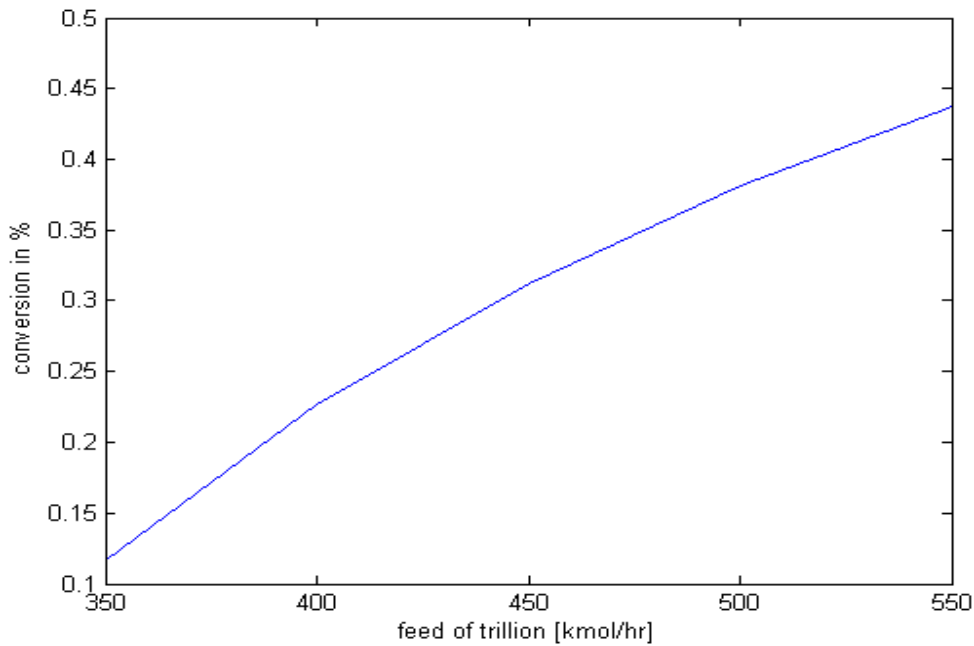


Figure 5.7. Variation of trillion conversions with trillion concentrations in the feed stream using equilibrium model

5.5.3. Effect of Feed Temperature

By varying the temperature of the feed streams, their effect on trillion conversions is studied. The feed temperature increases from 323K to 350K the conversion linearly increased. As shown from the figure 5.8. the conversion is constant as the temperature of the feed stream is changed from 350K to 410K. The trillion conversion is observed to be dependent of the feed stream temperature of trillion and methanol mixture.

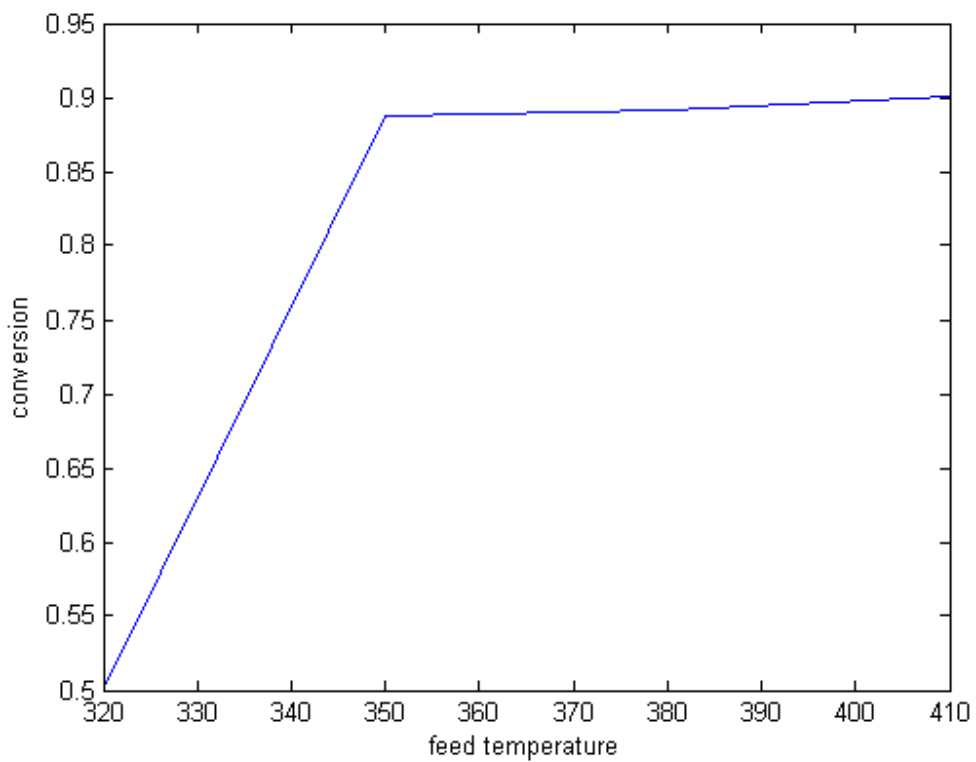


Figure 5.8. Effect of feed stream temperature on conversion.

5.6. Liquid and Vapor Flow Rate

The simulation result of liquid flow rate of the reactive distillation using equilibrium model is shown at figure 5.9. As shown from figure 5.9, the liquid flow rate increased along the height of the column due to the production of methyl linoleate and glycerol together. The flow rate of liquid from stage 1 to stage 2 linearly increased and it also increase slightly linear moved from stage 2 to stage 16. As shown from the figure 5.9 the liquid flow rate increased slightly exponentially as goes from stage 17 to the bottom of the column because of vapor flow rate is increased. The bottom product flow rate is 209.95 mol/s.

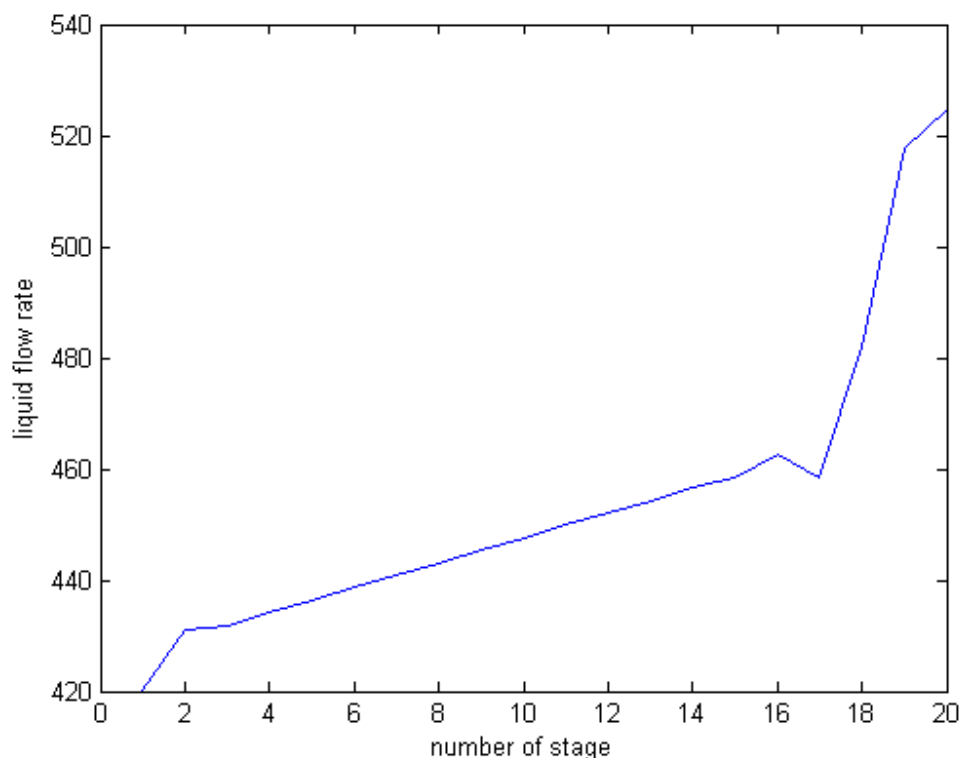


Figure 5.9. liquid flow rate along stage of the column

The vapor flow rate profile of the reactive distillation is shown at figure 5.10. As vapor flow rate is maximum at the bottom of the column because of highest amount of the liquid is boiled and reflux to the column. At stage 1, the vapor flow rate is maximum compare to the internal section of the column due to the condition of the feed flow rate is dominated by

vapor and then the vapor flow decreased to 122 mol/s at stage 2 because of high amount of liquid flow rate reflux to the column. As the factor of the methanol and trillion flow rate decreased, the vapor flow rate is increased from 122 mol/s (at stage 2) to 166 mol/s (at stage 16) and then the flow rate decreased to 160 mol/hr (at stage 17). As observed from the figure 5.10, the flow rate linearly increased with high slope as moved from stage 18 to bottom stage. The distillate flow rate is 140.05 mol/s.

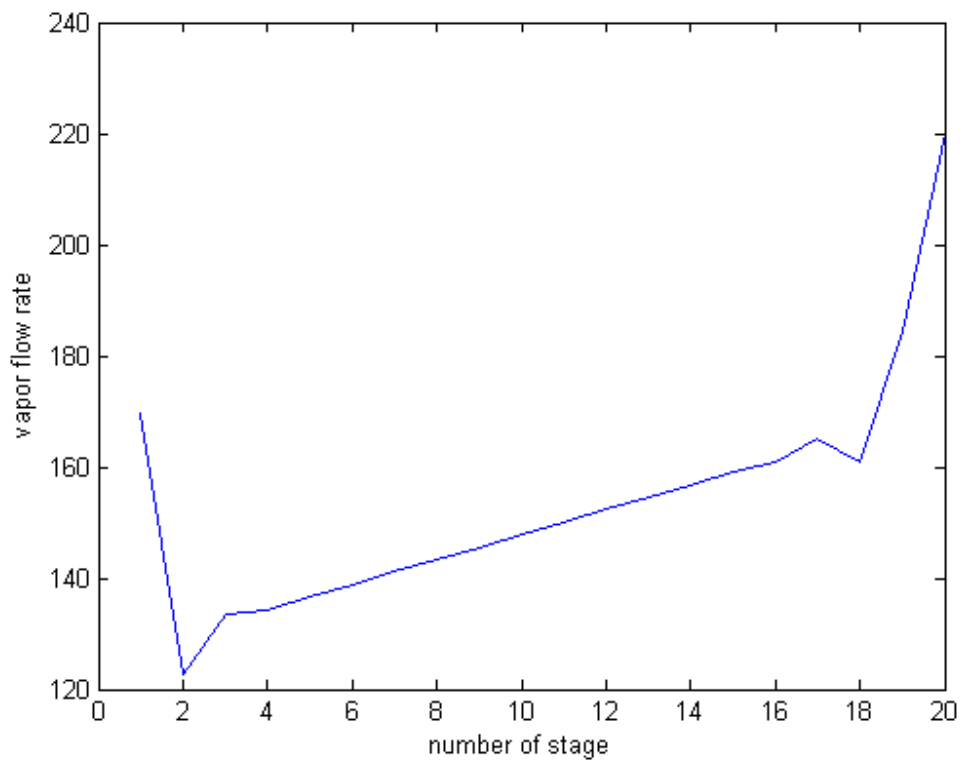


Figure 5.10. Vapor flow rate along stage of the column

6. CONCLUSION AND RECOMMENDATION

6.1. Conclusion

In this thesis, reactive distillation was studied to model and to simulate the biodiesel production from soybean oil.

The biodiesel processing was based on and compared to the conventional process of Zhang et al. (2003). In addition, three steps of reversible transesterification reaction which are triglyceride to diglyceride, diglyceride to monoglyceride and monoglyceride to glycerin were added for improving the calculation result.

The study covers development of a computer code for reactive distillation using MATLAB and its validation with Emile's work. It is also covers the study of the influence of feed concentration, reflux ratio and feed temperature on conversion with equilibrium model. The concentration and temperature profiles are also developed to show the column dynamics with the models.

A mathematical model for equilibrium model is developed for multi-component reactive distillation process. These models are solved numerically using a computer code developed using MATLAB program. Several M.files are written for calculation of the chemical kinetics, physical and thermodynamics properties.

The simulation results of the equilibrium model developed in the present work are validated using the data reported in the work of Emile.

After validation of the simulation results, parametric study has been carried out in the reactive distillation column using equilibrium model for temperature and concentration profiles using the system of biodiesel production, which is limited by equilibrium in a convention process.

Sensitivity analysis is carried out for reactive distillation column to see the effects of the trillion concentrations in the feed stream, reflux ratio and feed stream temperature.

The conversion of trillion is increase as its concentration in the feed stream increases, and is practically dependent of the feed stream temperature.

Reactive distillation is determined to be an attractive alternative to the conventional reaction- followed by distillation process strategies. Several promising advantages can be obtained especially those involving reduction of operating and investment costs, the overcoming of limitations imposed by chemical reaction equilibrium, benefits of heat integration obtained because the heat generated in the chemical reactions is used for vaporization, the suppression or elimination of unwanted side reactions (improved selectivity), beneficial effects of chemical reaction in reacting away some of the azeotropes in mixture and greatly simplifying the phase equilibrium behavior and reduction or elimination of reactant recycles.

6.2. Recommendation for Future Work

The following suggestions for future work can be considered:

1. Studying the non-equilibrium reactive distillation instead of the equilibrium reactive distillation.
2. Studying the reactive distillation instead of using energy balance using the empirical formula like Francis weir formula.
3. Simulating the dynamic state of equilibrium and non-equilibrium modeling of reactive distillation column.
4. Optimization of the reactive distillation.

Reference

1. Simasatitkul, L., et al., Reactive distillation for biodiesel production from soybean oil. Korean Journal of Chemical Engineering, 2011. 28(3): p. 649-655.
2. Hammond, E.G., et al., Soybean Oil, in Bailey's Industrial Oil and Fat Products, F. Shahidi, Editor. 2005. p. 577-604.
3. Warasak Limniyakul, Application of reactive distillation for biodiesel production enhancement. 2007: Kasetsart University.
4. Emilie Øritsland Houge, Modelling of the production of biodiesel by reactive distillation. 2012
5. Drapcho, C.M., N.P. Nhuan, and T.H. Walker, Biofuels Engineering Process Technology. 2008: McGraw-Hill.
6. Kiss, A.A. and C.S. Bildea, *A review of biodiesel production by integrated reactive separation technologies*. Journal of Chemical Technology & Biotechnology, 2012. **87**(7): p. 861-879.
7. Drapcho, C.M., N.P. Nhuan, and T.H. Walker, *Biofuels Engineering Process Technology*. 2008: McGraw-Hill.
8. Hauan.S., Hertzberg.T.,M.Lien.K.,(1996),”multiplicity in reactive distillation of MTBE”, Computers chem..Engng, Vol21, No.10, 1117-1124.
9. DIPPR 801 Databases. Available from: <http://dippr.byu.edu/students/>.
10. Asefaw Gezea, modeling of reactive distillation. 2004. Addis Ababa university.
11. Emilie Øritsland Houge, Reactive Distillation of Biodiesel Modeling and Optimal Operation. June 2013: Norwegian University of Science and Technology.
12. Knothe, G., J. Krahl, and J.V. Gerpen, *the Biodiesel Handbook*. 2 ed. 2010: AOCS Press.
13. Mathematical Modeling of a Two-Phase Bubble-Column Reactor for
14. Minhazuddin Mohammed, Biodiesel Production from Alternative Feedstocks. 2011. Drexel University.
15. Mohammed Z. Mohammed, mathematical modeling and simulation for production of MTBE by reactive distillation. 2003: University of Technology Chemical Engineering Department.

16. Mohd Usman Bin Mohd Junaidi, simulation of reactive distillation for biodiesel production from jatropha curcas seed oil. 2010.
17. Shyam Kumar, Modeling and Simulation of ethyl acetate reactive distillation column using ASPEN PLUS. 2010: ORISSA -769 008, India.
18. Obanifemi Aluko;dynamic modeling and control of reactive distillation for hydrogenation of benzene: August 2008
19. Seader.J.D.,Ernest Henley .J.,(1998), separation process principles ,John Wily and Sons, Inc..
20. Jhon, Y.H. and T.-h. Lee, *Dynamic simulation for reactive distillation with ETBE synthesis*. Separation and Purification Technology, 2003. **31**(3): p. 301-317.
21. *1-Monolinoleoyl-rac-glycerol*. Available from: <http://goo.gl/Ku39P>.
22. *1,2-dilinoleoylglycerol*. Available from: <http://goo.gl/45b0m>.
23. Reid, R.C., J.M. Prausnitz, and B.E. Poling, *The Properties of Gases & Liquids*. 4 ed. 1987: McGraw-Hill.
24. Issariyakul, T. and A.K. Dalai, *Comparative kinetics of transesterification for biodiesel production from palm oil and mustard oil*. The Canadian Journal of Chemical Engineering, 2012. **90**(2): p. 342-350.
25. Geankoplis, C.J., *Vapor-Liquid Separation Processes*, in *Transport Processes and Separation Process Principles*. 2003, Prentice Hall. p. 696-759.
26. Buckley, P.S., W.L. Luyben, and J.P. Shunta, *Design of Distillation Control Systems*. 1985: Edward Arnold.
27. Fredenslund, A., J. Gmehling, and P. Rasmussen, *vapor-liquid equilibria using UNIFAC*. 1977: Elsevier Scientific Publishing Company.
28. Anjan Srivastava and Ram Prasad, renewable and sustainable energy reviews. Volume 4, Issue 2, June 2000, page 111-133 F.Ma and M. Hanna, bioresource technology , volume 70, issue 1,October 1999, page 1-15.
29. Kiss A.A., Dimian A.C., Rothenberg G., 2007. Biodiesel Production by Integrated Reactive-Separation .Design. Computer Aided Chemical Engineering, 24, 1283-1288.
30. Behzadi, S., and Farid, M. M., 2009. Production of biodiesel using a continuous gas-liquid reactor. Bioresource technology 100:683.

31. Pisarenko, Yu. A; Serafimov, L.A; Cardona, C.A; Efremov, D.L; Shumalov, A.S.
Reactive Distillation Design: Analysis of the Process Statics. Reviews in chemical engineering. Inlaterra-Israel. Freunds pub, v.17, n.4, p.253 - 327, 2001.
(2001). Vol 17, No 4. p. 76.
32. Perry, R. H., and Green, D. W., "Perry's Chemical Engineering Handbook", 7th . Ed., McGraw-Hill, New York (1997).
33. 1-Monolinolein(2277-28-3). Available from: <http://goo.gl/zu4r9>.
34. 1,3-Dilinolein(15818-46-9). Available from: <http://goo.gl/UugMF>.
35. Velasco, S., et al., A predictive vapor-pressure equation. The Journal of Chemical Thermodynamics, 2008. **40**(5): p. 789-797.
36. Dennis Y.C. Leung , Xuan.Wu, and M. K. H. Leung, a review on biodiesel production using catalyzed transfesterification: 2006.
37. Ulf schuchardt, Ricardo sercheli, and Rogerio Matheus Vargas. Review transestrification of vegetable oils: may 9, 1997.
38. D.Kusdiana and S.Saka. Kinetics of transestrification in rape seed oil to biodiesel fuel as treated in supercritical methanol. April, 2001.
39. Gemma Vicente, Mercedes Martinez and Jose Aracil. Integerated biodiesel production: a comparison of different homogenous catalyts systems. May 2003.
40. A. stankiewicz. Reactive separations for process intensification: an industrial perspective: volume 42, issue 3, March 2003, page 137-144.
41. Agreeda., V. H., Partin L.R. and Hiese ,W.H. " High purity methyl acetate via reactive distillation," Chem. Eng. Progress,2,40-46 (1990).
42. Bravo,J.L.,A. pyhalthi and H. gaervelin "Investigation in Catalytic Distillation Pilot Plant : vapor-liquid equilibrium kinetics and mass transfer" issues Ind. Eng. Chem. 32,2220-2225 (1993).
43. Carra, S., E. Santacesaria, M. Morbidelli and L. Cavalli "synthesis of propylene oxide from propylene-chlorohydrins- II. Modeling of the distillation with chemical reaction unit", Chem. Eng. Sci. 34, 1133-1140 (1979).
44. Ciric, A.R., and Gu. D., synthesis of non-equilibrium reactive distillation by MINLP optimization, A.I.CH.J.40, 1479-1487 (1994).
45. Shoemaker, J.D. and E.M Jones Cumene by catalytic distillation, Hydrocarbon Process, June, 57-68 (1987).

46. *MATLAB Software version 7.0*, [.www.mathworks.com](http://www.mathworks.com).
47. Harvey, A. G., Irisay, G and Wozny, G. "Reactive Batch Distillation in Unconventional Column Configurations" Berlin University of Technology (2004).
48. Nouredini, H.; Zhu, D. Kinetics of Transesterification of Soybean Oil. *Journal of the American Oil Chemists' Society* 1997, 74 (11), 1457-1463.
49. Freedman, B.; Pryde, E. H.; Mounts, T. L. Variables affecting the yields of fatty esters from transesterified vegetable oils. *Journal of the American Oil Chemists' Society* 1984, 61(10), 1638-1643.
50. Cheirsilp, B.; H-Kittikun, A.; Limkatanyu, S. Impact of transesterification mechanisms on the kinetic modeling of biodiesel production by immobilized lipase. *Biochemical Engineering Journal* 2008, 42(3), 261-269.
51. King, C. J., *Separation Processes*, McGraw-Hill, New York (1980).
52. Kister, H. Z., *Distillation Design*, McGraw-Hill, New York (1992).
53. S. Skogestad and I. Postlethwaite, Wiley, Chichester, U.K., *Multivariable feedback control analysis and design*, ISBN 0-471-94277-4, 559, 1996.
54. Luyben, W. L. Derivation of Transfer Functions for Highly Nonlinear Distillation Columns. *Ind. Eng. Chem. Res.* 1987, 26, 2490-2495.
55. Gilliland, E.R. and Reed, C.E., "Degree of Freedom in Multi-component Absorption and Rectification.", *Ind. Eng. Chem.*, 34, 551-557 (1942).
56. KWAUK, I.: A. 1. Ch. E. Journal 2,240 (1956).

APPENDICES

A: Matlab Scripts

This appendix gives a print of the Matlab files that constitute the steady state model.

A.1 The main file

The main script is given below, and mainly contains specifications for the simulation.

```
%Basic model for reactive distillation column for biodiesel production
```

```
%clc, clear all, close all
```

```
Format long
```

```
%Feed flows
```

```
% metOH/TG/DG/MG/GL/BD
```

```
FF =[300 50 0 0 0 0];
```

```
F0 = 350;% total feed rate
```

```
z =[300/350 50/350 0 0 0 0];
```

```
Vr= 350;
```

```
rD =3; % reflux ratio
```

```
rB =4 ; % reboiler ratio
```

```
Ds = 140.05; % Distillate [kmol/h]
```

```
Bt = 209.95; %Bottot =ms, [kmol/h
```

```
R =8.314; % ideal gas constant
```

```
Mw = [32.0 879.3844 616.95 354.52 92.094 294.47]; %Molecular weights  
[kg/kmol];
```

```
% relative volatility of each component
```

```
alpha = [1 0.01 0.01 0.02 0.05 0.03];
```

```
%antoine constants
```

```
AA =[82.718 234.71 -15.931 118.95 99.986 105.4];
```

```
BB = [-6.9045*103 -3.4699*104 -2111 -2.0181*104 -1.3808*104 -  
1.4531*104];
```

```
CC =[ -8.8622 -27.25 2.4303 -14.32 -10.088 -10.986];
```

```
DD =[5.8959*10-19 3.18337*10-20 1.74025*10-18 1.79996*10-18 1.14067*10-5  
4.61746*10-6];
```

```
EE =[6 6 6 6 2 2];
```

```
for K=1:12
```

```
% intial liquid composition
```

```
    x(1,:)= [1.0000 1.656e-24 7.9e-8 1.294e-8 2.784e-5 4.972e-6];
```

```
    x(2,:)= [0.6909 1.133e-2 5.203e-3 5.958e-3 6.738e-2 0.2192];
```

```
    x(3,:)= [0.6486 2.367e-3 2.650e-3 2.785e-3 8.386e-2 0.2598];
```

```
    x(4,:)= [0.6412 1.131e-3 1.905e-3 2.002e-3 8.696e-2 0.2668];
```

```
    x(11,:)= [0.6398 9.082e-4 1.730e-3 1.823e-3 8.761e-2 0.2682];
```

```
    x(20,:)= [0.3408 1.760e-3 3.306e-3 3.434e-3 0.1601 0.4906];
```

```
    for i=5:n-10
```

```
        x(i,:)=x(4,:);
```

```
    end
```

```
    for i=12:n-1
```

```
        x(i,:)=x(11,:);
```

```
    end
```

```
% normalization of intila composition
```

```
    Sum = zeros(n,c);
```

```
    for i=1:c
```

```

        for j=1:n
            Sum(j,i) = Sum(j,i)+ x(j,i);
        end
    end
    for i=1:c
        for j=1:n
            Xn(j,i) = x(j,i)/Sum(j,i);
        end
    end
    end
    %The boiling points for the respective components [K]:
    Tb = [337.63 1199.65 922.35 696.35 561.0 653.15];
    % relative volatility of each component
    alpha = [1 0.01 0.01 0.02 0.05 0.03];
    % Setting the initial temperature
    % calculating intial temperature using boiling point temperatures
    for i=1:n
        for j=1:c
            TT(i,j)=Xn(i,j)*Tb(j);
        end
    end
    end
    % intial liquid flow rates
    V(1)= (rD+1)*Ds;
    for i=2:n-2
        V(i)=V(i-1)+(q-1)*F0;
    end
    V(n)=(rB*Bt);
    % intial vapor flow rate
    L(1)= rD*Ds;
    for i=2:n-1
        L(i)=V(i+1)-V(1)-Ds+F0;
    end
    L(n)=Bt;
    sum =zeros(n,c);
    for i=1:n
        for j=1:c
            sum(i,j) = sum(i,j)+(Xn(i,j)*alpha(j));
        end
    end
    for i=1:n
        for j=1:c
            y(i,j)=(alpha(j)/((sum(i,j)))*x(i,j));
            l(i,j)= x(i,j)*L(j) ;
        end
    end
    v(i,j)=y(i,j)*V(j);
    end
    end
    for i=1:n
        for j=1:c
            k(i,j)= y(i,j)/Xn(i,j);
        end
    end
    end
    % Calculation of the kinetics in the liquid phase:
    % The sizes of the kinetic constants:
    k1 = ones(n,1); k2 = ones(n,1); k3 = ones(n,1);
    k4 = ones(n,1); k5 = ones(n,1); k6 = ones(n,1);
    % for i = 1:n
    %Kinetic data for the reaction
    k1(i) = 3.9*3600*(10^7)*exp(-54.9987\ (R*T(i,1))); %rate constants [m3/kmol*h]

```

```

k2(i) = 5.78*3600*(10^5)*exp(-41.5555/(R*T(i,1)));
k3(i) = 5.906*3600*(10^12)*exp(-83.0942/(R*T(i,1)));
k4(i) = 9.888*3600*(10^9)*exp(-61.2496/(R*T(i,1)));
k5(i) = 5.335*3600*(10^3)*exp(-26.8655/(R*T(i,1)));
k6(i) = 2.1*3600*(10^4)*exp(-40.1162/(R*T(i,1)));
end
%The reactions. R is the gain/loss in [kmol/h]
for i= 1:n-1
R_TG = -((k1(i+1)*x(i,2)*x(i,1)) - (k2(i+1)*x(i,3)*x(i,6)))*(Mw(1)*Vr);
R_DG = ((k1(i+1)*x(i,2)*x(i,1)) - (k2(i+1)*x(i,3)*x(i,6)) +
(k3(i+1)*x(i,3)*x(i,1)) + (k4(i+1)*x(i,4)*x(i,6)))*(Mw(2));
R_MG = ((k3(i+1)*x(i,3)*x(i,1)) - (k4(i+1)*x(i,4)*x(i,6)) -
(k5(i+1)*x(i,4)*x(i,1)) + (k6(i+1)*x(i,5)*x(i,6)))*(Mw(3));
R_BD = ((k1(i+1)*x(i,2)*x(i,1)) -
(k2(i+1)*x(i,3)*x(i,6)) + (k3(i+1)*x(i,3)*x(i,1)) -
(k4(i+1)*x(i,4)*x(i,6)) + (k5(i+1)*x(i,4)*x(i,1)) + (k6(i+1)*x(i,5)*x(i,6)))*(Mw(
4));
R_GL = ((k5(i+1)*x(i,4)*x(i,1)) + (k6(i+1)*x(i,5)*x(i,6)))*(Mw(5)/Vr);
R_MetOH = ((k1(i+1)*x(i,2)*x(i,1)) + (k2(i+1)*x(i,3)*x(i,6)) -
(k3(i+1)*x(i,3)*x(i,1)) - (k4(i+1)*x(i,4)*x(i,6)) - (k5(i+1)*x(i,4)*x(i,1)) -
(k6(i+1)*x(i,5)*x(i,6)))*Vr);
%We store the molar gain of each component in an R matrix:
R(i,1) = R_MetOH; R(i,2) = R_TG; R(i,3) = R_DG; R(i,4) = R_MG
R(i,5) = R_GL; R(i,6) = R_BD;
R = [R_MetOH; R_TG ; R_DG ; R_MG; R_GL; R_BD];
end
%for component mtOH
A1(1) = 0;
B1(1) = -V(1)*k(1,1) - L(1);
C1(1) = V(2)*k(1,2);
E1(1) = 0;
A1(n) = L(n-1);
B1(n) = -(V(n)*k(n,1) + Bt);
C1(n) = 0;
E1(n) = 0;
for j=2:n-1
A1(j) = L(j-1);
B1(j) = -L(j) - V(j)*k(j,1);
C1(j) = -V(j)*k(j+1,1);
E1(j) = -FF(1)*z(1) - R_MetOH;
end
% thomas algorithm
C1(1) = C1(1)/B1(1);
E1(1) = E1(1)/B1(1);
for i=2:n-1
temp = B1(i) - A1(i)*C1(i-1);
C1(i) = C1(i)/temp;
E1(i) = (E1(i) - A1(i)*E1(i-1))/temp;
end
E1(n) = (E1(n) + A1(n)*E1(n-1))/(B1(n) - A1(n)*C1(n-1));
x1(n) = E1(n-1);
for i = n-1:-1:1
x1(i) = 1 - E1(i) - C1(i)*x1(i+1);
end
%for component TG
A2(1) = 0;
B2(1) = -V(1)*k(1,2) - L(1);

```

```

C2(1)=V(2)*k(2,2);
E2(1)=0;
A2(n)=L(n-1);
B2(n)=- (V(n)*k(n,2)+Bt);
C2(n)=0;
E2(n)=0;
for j=20:n
    A1(j)=L(j-1);
    B1(j)=- (V(j)*k(j,1)+Bt);
    C1(j)=0;
end

for j=2:n-1
    A2(j)=L(j-1);
    B2(j)=-L(j)-V(j)*k(j,2);
    C2(j)=-V(j)*k(j+1,2);
    E2(j)=-FF(2)*z(2)-R_TG;
end
% thomas algorithm
C2(1)=C2(1)/B2(1);
E2(1)=E2(1)/B2(1);
for i=2:n
    temp = (-B2(i)+A2(i)*C2(i-1));
    C2(i) = C2(i)/temp;
    E2(i) = (E2(i)+A2(i)*E2(i-1))/-temp;
end
E2(n) = (E2(n)-A2(n)*E2(n-1))/(B2(n)-A2(n)*C2(n-1));
x2(n)=E2(n-1);
for i = n-1:-1:1
    x2(i) = E2(i)-C2(i)*x2(i+1);
end
%for component DG
A3(1)= 0;
B3(1)=-V(1)*k(1,3)-L(1);
C3(1)=V(2)*k(2,3);
E3(1)=0;
A3(n)=L(n-1);
B3(n)=- (V(n)*k(n,3)+Bt);
C3(n)=0;
E3(n)=0;
for j=2:n-1
    A3(j)=L(j-1);
    B3(j)=-L(j)-V(j)*k(j,3);
    C3(j)=V(j)*k(j+1,3);
    E3(j)=-FF(3)*z(3)-R_DG/Vr;
end
% thomas algorithm
C3(1)=C3(1)/B3(1);
E3(1)=E3(1)/B3(1);
for i=2:n-1
    temp = B3(i)-A3(i)*C3(i-1);
    C3(i) = C3(i)/temp;
    E3(i) = (E3(i)-A3(i)*E3(i-1))/temp;
end
E3(n) = (E3(n)-A3(n)*E3(n-1))/(B3(n)-A3(n)*C3(n-1));
x3(n)=E3(n);
for i = n-1:-1:1

```

```

        x3(i) = E3(i) - C3(i) * x3(i+1);
end
%for component MG
A4(1) = 0;
B4(1) = -V(1) * k(1, 4) - L(1);
C4(1) = V(2) * k(2, 4);
E4(1) = 0;
A4(n) = L(n-1);
B4(n) = -(V(n) * k(n, 4) + Bt);
C4(n) = 0;
E4(n) = 0;
for j = 2:n-1
    A4(j) = L(j-1);
    B4(j) = -L(j) - V(j) * k(j, 4);
    C4(j) = V(j) * k(j+1, 4);
    E4(j) = -FF(4) * z(4) - R_MG/Vr;
end
% thomas algorithm
C4(1) = C4(1) / B4(1);
E4(1) = E4(1) / B4(1);
for i = 2:n-1
    temp = B4(i) - A4(i) * C4(i-1);
    C4(i) = C4(i) / temp;
    E4(i) = (E4(i) - A4(i) * E4(i-1)) / temp;
end
E4(n) = (E4(n) - A4(n) * E4(n-1)) / (B4(n) - A4(n) * C4(n-1));
x4(n) = E4(n);
for i = n-1:-1:1
    x4(i) = E4(i) - C4(i) * x4(i+1);
end
%for component GL
A5(1) = 0;
B5(1) = -V(1) * k(1, 5) - L(1);
C5(1) = V(2) * k(2, 5);
E5(1) = 0;
A5(n) = L(n-1);
B5(n) = -(V(n) * k(n, 5) + Bt);
C5(n) = V(n);
E5(n) = 0;
for j = 2:n-1
    A5(j) = L(j-1);
    B5(j) = -L(j) - V(j) * k(j, 5);
    C5(j) = V(j) * k(j+1, 5);
    E5(j) = -FF(5) * z(5) - R_GL * Vr;
end
% thomas algorithm
C5(1) = C5(1) / B5(1);
E5(1) = E5(1) / B5(1);
for i = 2:n-1
    temp = B5(i) - A5(i) * C5(i-1);
    C5(i) = C5(i) / temp;
    E5(i) = (E5(i) - A5(i) * E5(i-1)) / temp;
end
E5(n) = (E5(n) - A5(n) * E5(n-1)) / (B5(n) - A5(n) * C5(n-1));
x5(n) = E5(n);
for i = n-1:-1:1
    x5(i) = E5(i) - C5(i) * x5(i+1);

```

```

end
%for component BD
A6(1)= 0;
B6(1)=-V(1)*k(1,6)-L(1);
C6(1)=-V(2)*k(2,6);
E6(1)=0;
A6(n)=L(n-1);
B6(n)=- (V(n)*k(n,1)+Bt);
C6(n)=0;
E6(n)=0;
for j=2:n-1
    A6(j)=L(j-1);
    B6(j)=L(j)-V(j)*k(j,6);
    C6(j)=V(j)*k(j+1,6);
    E6(j)=-FF(6)*z(6)-R_BD*Vr/(Mw(6));
end
% thomas algorithm
C6(1)=C6(1)/B6(1);
E6(1)=E6(1)/B6(1);
for i=2:n-1
    temp = B6(i)-A6(i)*C6(i-1);
    C6(i)= C6(i)/temp;
    E6(i)= (E6(i)-A6(i)*E6(i-1))/temp;
end
E6(n)=(E6(n)-A6(n)*E6(n-1))/(B6(n)-A6(n)*C6(n-1));
x6(n)=E6(n-1);
for i = n-1:-1:1
    x6(i)= E6(i)-C6(i)*x6(i+1);
end
X1=[x1; x2; x3; x4; x5; x6]';
% temperature
%bubble point calculation using feed composition
x_met = 6/7;
x_TG = 1/7;
A_met = 82.718;
B_met = -6.9045*10^3;
C_met = -8.8622;
D_met = 7.4664*10^-6;
E_met = 2;
A_TG = 234.71;
B_TG = -3.4699*10^4;
C_TG = -27.25;
D_TG = 1.5475*10^-18;
E_TG = 6;
for Tt = 323.15:0.001:1000
    Temp(1,1) = Tt;
    P_met(1,1) = 9.869*(10^-6)*exp(A_met + (B_met/Tt) + (C_met*log(Tt))
    +(D_met*Tt^E_met));
    P_TG(1,1) = 9.869*(10^-6)*exp(A_TG + (B_TG/Tt) + (C_TG*log(Tt))
    +(D_TG*Tt^E_TG));
    P(1,1) = (x_met*P_met(1,1))+(x_TG*P_TG(1,1));
    e(1,1) = 1-P(1,1); %The error from the actual pressure of 1 atm
    if (e(1,1) <= 0.0001 && e(1,1) >= 0)
        disp([Tt]);
        break
    else i = i+1;
        Tt = Tt + 0.01;
    end
end

```

```

end
end
for i=1:c
    TT(i) = (BB(i) / (AA(i) - log(P))) - CC(i);
    psat(i) = AA(i) - (BB(i) / TT(i) + CC(i));
end
g = psat/psat(1); r = g*X1; G = zeros(1,n);
for i=1:c
    for j=1:n
        g = psat/psat(1);
        r = g*X1;
        Sum = G+r;
        Pj = p \ Sum;
    end
end
for j=1:c
    T(j) = (BB(j) / (-AA(j) - log(Pj(j)))) - CC(j);
end
% vapor enthalpy calculation
Ap = [9.2969 0 0 7.8468 2.5604 2.2999];
Bp = [2.692 0 0 1.1067 -2.7414 9.924];
Cp = [-4.4542 0 0 0 1.4777*10 6.7574];
Dp = [0 0 0 0 -3.5078*10^-2 0];
Ep = [0 0 0 0 3.2719*10^-5 0];
% liquid and vapour heat capacity
for i=1:c
    cpl(i) = Ap(i) + Bp(i) * Tt + Cp(i) * Tt^2;
    cpv(i) = Ap(i) + Bp(i) * Tt + Cp(i) * Tt^2 + Dp(i) * (Tt^3);
    cpf(i) = Ap(i) + (Bp(i) * Tf(i)) + Cp(i) * Tf(i).^2;
end
hl = zeros(c); hv = zeros(c); hf = zeros(c);
for i=1:c
    Tr(i) = Tt / Tc(i);
    hv(i) = x1(i) * (Hf(i) + cpv(i) * (Tt - Tr(i)));
    hf(i) = z(i) * (Hf(i) + cpf(i) * (Tf(i) - Tr(i)));
    hl(i) = hl(i) + y(n,i) * (Hf(i) + cpl(i) * (Tt - Tr(i)));
    hll(i) = hl(i,1);
end
h = zeros(1,n); H = zeros(1,n);

for j=1:n
    for i=1:c
        h(j) = h(1,j) + V(j) * hv(i);
        H(j) = H(1,n) + L(j) * hll(i);
    end
end

HD = hv(1) * Ds * X1(1,i); % distillate enthalpy
Hfeed = FF(i) * hf(i); % feed enthalpy
Qc = FF(1) * h(7) + v(2) * H(2) - v(1) * H(1) - (l(1) + Ds) * h(1); % condenser heat duty
Qr = F0 * h(7) - V(1) * H(1) - L(n) * h(n); % boiler heat duty
for j=2:n-1
    alp(j) = h(j-1) - H(j) / (10^12);
    beta(j) = H(j+1) - h(j) / (10^12);
    gamma(j) = (F0 * R(1)) * h(j) / (10^12);
end

```

```

alp(n)=1;
gamma(20)= rB*Bt;

%for diadiagonal matrix solver
for j=2:n
    A11(j)=alp(j);
    C11(j)=0;
    B11(j)= beta(j-1) ;
    E11(j)=gamma(j);
end
% thomas algorithm
E11(1)=E11(1)/B11(1);
for i=2:n-1
    temp = B11(i)-A11(i)*C11(i-1);
    C11(i)= C11(i)/temp;
    E1(i)= (E1(i)-A11(i)*E11(i-1))/temp;
end
E11(n)=(E11(n)-A11(n)*-E11(n-1))/(-B11(n)-A11(n)*C11(n-1));
V1(1)=E11(2)
V1(n)=E11(n-1);
for i = n-1:-1:2
    V1(i)= E11(i)-C1(i)*V1(i+1);
end
D =(V(2)/(rD+1));
L1(1)=rD*D;
for i=2:n-1
    L1(i)=V1(i+1)-V1(1)-D+F0+R(1);
    L1(n)=Bt;
end
while (V(K)-V1(K+1))>=0.0000001)
    V(K)=V1(K);
    L(K)=L1(K);
end
end

```

B: Estimation of Critical Temperatures and Pressures

The critical temperatures and pressures were estimated according to the Joback method as described in chapter 3 [22].

B.1. The Joback Method

The Joback method is a group contribution method. This means that it will estimate critical properties of pure compounds based on the functional groups in the molecule. The Joback method allows for fast and easy estimations of critical properties, but it does not have the greatest accuracy for all compounds. The Joback method is one of the recommended methods for application when a reliable value for the boiling point is available [22].

The equations for the critical temperatures and pressures are given below as equations B.1 and B.2 [22].

$$T_c = T_b[0.584 + 0.965 \sum \Delta T - (\sum \Delta T)^2]^{-1} \quad (\text{B-1})$$

$$P_c = (0.113 + 0.0032N_A - \sum \Delta P)^{-2} \quad (\text{B-2})$$

The parameters ΔT and ΔP are the functional group contribution values to the critical temperature and pressures and are given in Table B.1 below, while N_A is the number of atoms present in the molecule. Table B.1 also contains the number of said functional groups that are present in the monolinolein and dilinolein molecules.

Table B-1: Group contributions to T_c and P_c .

Functional group	T_c	P_c	Number of groups in DG	Number of groups in MG
-CH ₃	0.0141	-0.0012	2	1
-CH ₂ -	0.0189	0	26	14
-CH=	0.0129	-0.0006	8	4
-COO-	0.0481	0.0005	2	1
-CH<	0.0164	0.002	1	1
-OH	0.0741	0.0112	1	2

The calculation for ΔT and ΔP for MG and DG are shown below:

$$\Delta T[\text{DG}] = 2(0.0141) + 26(0.0189) + 8(0.0129) + 2(0.0481) + 0.0164 + 0.0741 = 0.8095$$

$$\Delta T[\text{MG}] = 0.0141 + 14(0.0189) + 4(0.0129) + 0.0481 + 0.0164 + 2(0.0741) = 0.543$$

$$\Delta P[\text{DG}] = 2(-0.0012) + 8(-0.0006) + 2(0.0005) + 0.002 + 0.0112 = 0.007$$

$$\Delta P[\text{MG}] = -0.0012 + 4(-0.0006) + 0.0005 + 0.002 + 2(0.0112) = 0.0213$$

By applying equations B-1 and B-2 as well as the boiling point of DG and MG that are given in table 3.4, the critical temperature and pressure were estimated:

$$T_c [\text{DG}] = 942.57[0.584 + 0.965(0.8095) - (0.8095)^2]^{-1} = 1327.79\text{K}$$

$$T_c [\text{MG}] = 758.2[0.584 + 0.965(0.543) - (0.543)^2]^{-1} = 932.43\text{K}$$

$$P_c \text{ [DG]} = (0.113 + 0.0032(112) - 0.007)^{-2} = 4.6368\text{Pa}$$

$$P_c \text{ [MG]} = (0.113 + 0.0032(63) - 0.0213)^{-2} = 11.625 \text{ Pa}$$

C: Bubble Point Estimations

This is an overview of the calculations for the bubble point temperatures and enthalpies, so that the liquid feed fraction could be estimated.

C.1. Parameters

The necessary parameters for the calculation are given below: $A_{\text{met}} = 82.718;$

```
B_met = -6.9045*10^3;  
C_met = -8.8622;  
D_met = 7.4664*10^-6;  
E_met = 2;  
A_TG = 234.71;  
B_TG = -3.4699*10^4;  
C_TG = -27.25;  
D_TG = 1.5475*10^-18;  
E_TG = 6;
```

This represents the parameters for the vapour pressure equations derived from the DIPPR project 801 database for methanol and trilinolein in the feed.

The bubble point was estimated using an iterative method applying Raoult's law:

1. An initial value for the temperature was set.
2. The vapour pressure was calculated for all components present.
3. The total pressure was calculated, with the liquid fractions being equal to the composition of the feed.
4. The difference between the actual pressure and the calculated pressure was estimated
5. If the difference is too large, re-estimate T and continue steps 2-4 until convergence has been achieved.

Calculation - Temperature

This is a copy of the Matlab script written.

```
x_met = 6/7;x_TG = 1/7;
```

The molar fractions of the feed are stated. The iteration for the bubble point temperature is given in a for-loop:

```
for Tt = 323.15:0.001:1000
Temp(1,1) = Tt;
P_met(1,1) = 9.869*(10^-6)*exp(A_met + (B_met/Tt) + (C_met*log(Tt))
+(D_met*Tt^E_met));
P_TG(1,1) = 9.869*(10^-6)*exp(A_TG + (B_TG/Tt) + (C_TG*log(Tt))
+(D_TG*Tt^E_TG));
P(1,1) = (x_met*P_met(1,1))+(x_TG*P_TG(1,1));
e(1,1) = 1-P(1,1); %The error from the actual pressure of 1 atm
if (e(1,1) <= 0.0001 && e(1,1) >= 0)
disp([Tt]);
break
else i = i+1;
Tt = Tt + 0.01;
end
end
```

Here the first temperature to satisfy the demands with an error of 0.0001 is recorded and stored. The bubble point temperature obtained is 341.65K

Enthalpy

The heats of formation and heats of vaporisation for methanol and trilinolein are given in Table C-1 below. The values are from the DIPPR 801 database. An intermediate value was used for the liquid heat capacity.

Table C-1: The heats of formation and heat of condensation for methanol and trillion

	MetOH[J/mol]	TG[J/mol]
$\Delta H_f[298.15]$	-239100	-1748000
	-37460	-221070
	86.158	1745.05

The calculations as follow:

$$\Delta H_{\text{MetOH}}[298.15-341.65] = \sum cp \cdot \Delta T = 3747.87$$

$$\Delta H_{\text{MetOH}}[341.65] = \Delta H_f - \Delta H_{\text{vap}} + \sum cp \cdot \Delta T = -272812.12$$

$$\Delta H_{\text{TG}}[298.15-341.65] = \sum cp \cdot \Delta T = 75909.675$$

$$\Delta H_{\text{TG}}[341.65] = \Delta H_f - \Delta H_{\text{vap}} + \sum cp \cdot \Delta T = -1893160.3$$

Combining the enthalpies with the molar fractions, the enthalpy at the bubble point is calculated:

$$\Delta H [341.65] = x_{\text{MetOH}} \cdot \Delta H_{\text{MetOH}} + x_{\text{TG}} \cdot \Delta H_{\text{TG}} = -504290.44 \text{ J/mol}$$

D. Estimation of Vapor Pressure Equations

The vapor pressure equations for monolinolein and dilinolein were estimated according to a modified Clausius-Clapeyron equation, the Riedel equation. The Riedel method for estimating vapor pressures is fairly accurate for pure compounds, but validity is lower when approaching lower temperatures and pressures. The equation is given below as number D.1, and gives the vapor pressure in Pa [35].

$$\ln(P_r) = A - \frac{B}{T_r} + C \cdot \ln(T_r) + D \cdot T_r^6 \quad \text{D-1}$$

Here the first three terms represent the integration of the Clausius-Clapeyron equation, while the last term was added by Riedel to reduce inaccuracies. The reduced pressure and reduced temperature is defined as shown in equations D.2 and D.3 [35].

$$P_r = \frac{P^*}{P_c} \quad \text{D-2}$$

$$T_r = \frac{T}{T_c} \quad \text{D-3}$$

By algebraic manipulation of equations D.2 and D.3 one can get an expression for P^* and T . These can be substituted into equation D.1 and then a vapour pressure equation dependent on the system temperature has been derived:

$$P^* = \exp\left(A - \frac{B}{T_r} + C \cdot \ln(T_r) + D \cdot T_r^6\right) \quad \text{D-4}$$

The constants of equation D-4 are defined as [35]:

$$A = -35Q, B = -36Q, C = 42Q + \alpha_c, D = -Q$$

To calculate the constants, one needs to obtain the variables α_c and Q. The constant is an empirical parameter found from correlations in vapor pressure experimental data. To obtain α_c , and in turn Q, one must first equate T_{br} , P_{br} and ψ_b :

$$T_{br} = \frac{T_b}{T_c} \quad \text{D-5}$$

$$P_{br} = \frac{0.1013}{P_c} \quad \text{D-6}$$

$$\psi_b = -35 + \frac{36}{T_{br}} + 42 \cdot \ln(T_{br}) - T_{br}^6 \quad \text{D-7}$$

$$\alpha_c = \frac{K_1 K_2 \psi_b - \ln(P_{br})}{K_1 \psi_b - \ln(T_{br})} \quad \text{D-8}$$

$$Q = K_1(K_2 - \alpha_c) \quad \text{D-9}$$

The values of K_1 and K_2 are 0.0838 and 3.758 respectively. Once all of these constants are derived, one can substitute them into equation D.4 and get an expression for the vapour pressure.

D.1. The Calculation- Dilinolein

The first step was to calculate the values for T_{br} and P_{br} :

$$T_{br} = \frac{942.6}{1327.8} = 0.7099 \quad \text{and} \quad P_{br} = \frac{0.1013}{0.46368} = 0.21852$$

Next the values of ψ_b

$$\psi_b = -35 + \frac{36}{0.7099} + 42 \cdot \ln(0.7099) - 0.7099^6 = 1.19287$$

$$\alpha_c = \frac{0.0838 \cdot 3.758 \cdot 1.19287 - \ln(0.21852)}{0.0838 \cdot 1.19287 - \ln(0.7099)} = 4.2850$$

$$Q = 0.0838(3.758 - 4.2850) = -0.04416$$

The α_c and Q were then used to calculate the constants A, B, C and D:

$$A = -35(-0.04416) = 1.5457, B = -36(-0.04416) = 1.5898$$

$$C = 42(-0.04416) + 4.2850 = 2.4303, D = -(-0.04416) = 0.04416$$

Insert into equation D-4, we get

$$P^*[DG] = \exp \left(1.5457 - \frac{1.5898(1327.8)}{T} + 2.4303 \cdot \ln(T) - \ln(1327.8) + \frac{0.04416 \cdot T^6}{1327.8^6} \right)$$

$$P^*[DG] = \exp \left(-15.9313 - \frac{2111}{T} + 2.4303 \cdot \ln(T) + 8.0567 \cdot 10^{-2} \cdot T^6 \right)$$

D.2. The calculation - Monolinolein

The first step was to calculate the values for T_{br} and P_{br} :

$$T_{br} = \frac{758.2}{932.43} = 0.8131 \text{ and } P_{br} = \frac{0.1013}{1.1625} = 0.0871$$

Next the values of ψ_b

$$\psi_b = -35 + \frac{36}{0.8131} + 42 \cdot \ln(0.8131) - 0.8131^6 = 0.29617$$

$$\alpha_c = \frac{0.0838 \cdot 3.758 \cdot 0.29617 - \ln(0.087161)}{0.0838 \cdot 0.29617 - \ln(0.8131)} = 10.9324$$

$$Q = 0.0838(3.758 - 10.9324) = -0.60121$$

The α_c and Q were then used to calculate the constants A, B, C and D:

$$A = -35(-0.60121) = 21.0425, B = -36(-0.60121) = 21.6436$$

$$C = 42(-0.60121) + 10.9324 = -14.3184, D = -(-0.60121) = 0.60121$$

Insert into equation D-4, we get:

$$P^*[MG] = \exp \left(21.0425 - \frac{21.6436(932.43)}{T} - 14.3184 \cdot \ln(T) - \ln(932.43) + \frac{0.60121 \cdot T^6}{932.43^6} \right)$$

$$P^*[MG] = \exp \left(118.9488 - \frac{20181.142}{T} - 14.3184 \cdot \ln(T) + 9.1481 \cdot 10^{-19} \cdot T^6 \right)$$